Evaluation of the inhibitory activity of (aza)isoindolinone-type compounds: toward in vitro InhA action, Mycobacterium tuberculosis growth and mycolic acid biosynthesis

Aurélien Chollet, Jean-Luc Stigliani, Maria Rosalia Pasca, Giorgia Mori, Christian Lherbet, Patricia Constant, A. Quemard, Jean Bernadou, G. Pratviel, Vania Bernardes-Génisson

Received Date : 18-Feb-2016
Revised Date : 06-Jun-2016
Accepted Date : 11-Jun-2016
Article type : Research Article

Evaluation of the inhibitory activity of (aza)isoindolinone-type compounds: Towards *in vitro* InhA action, *Mycobacterium tuberculosis* growth and mycolic acid biosynthesis

Short running title: (Aza)isoindolinone-type derivatives: evaluation towards *in vitro* InhA action, *Mycobacterium tuberculosis* growth and mycolic acid biosynthesis

Keywords: (aza)isoindolinone, InhA inhibition, docking, *Mycobacterium tuberculosis,* structure-activity relationship, mycolic acid biosynthesis.

Aurélien Chollet,[a,b,c,d] Jean-Luc Stigliani,[a,b] Maria Rosalia Pasca,[e] Giorgia Mori[e], Christian Lherbet,[c,d] Patricia Constant,[f,g] Annaïk Quémard,[f,g] Jean Bernadou,[a,b] Geneviève Pratviel,[a,b] Vania Bernardes-Génisson*[a,b]

[a]Laboratoire de Chimie de Coordination (LCC), Centre National de la Recherche Scientifique (CNRS), BP 44099, 205 Route de Narbonne, F-31077, Toulouse, Cedex 4, France
[b]Université de Toulouse, Université Paul Sabatier, INPT, F-31077, Toulouse, Cedex 4, France
[c]Laboratoire de Synthèse et Physicochimie de Molécules d'Intérêt Biologique (SPCMIB), Centre National de la Recherche Scientifique (CNRS), 118 Route de Narbonne, 31062, Toulouse, Cedex 9, France
[d]Université de Toulouse, Université Paul Sabatier, LSPCMIB, F-31077, Toulouse, France
[e]Dipartimento di Biologia e Biotecnologie "Lazzaro Spallanzani", via Ferrata 1, 27100 Pavia, Italy.
[f]Institut de Pharmacologie et de Biologie Structurale (IPBS), Centre National de la Recherche Scientifique (CNRS), BP 64182, 205 Route de Narbonne, F-31077, Toulouse, France

[g]Université de Toulouse, Université Paul Sabatier, IPBS, F-31077, Toulouse, France

Corresponding author: Vania Bernardes-Génisson, vania.bernardes-genisson@lcc-toulouse.fr

Abstract

Inhibitors of the *Mycobacterium tuberculosis* enoyl-ACP reductase (InhA) are considered as potential promising therapeutics for the treatment of tuberculosis. Previously, we reported that azaisoindolinone-type compounds displayed, *in vitro,* inhibitory activity towards InhA. Herein we describe chemical modifications of azaisoindolinone scaffold, the synthesis of 15 new compounds and their evaluations toward the *in vitro* InhA activity. Based on these results, a structure–InhA inhibitory activity relationship analysis and a molecular docking study, using the conformation of InhA found in the 2H7M crystal structure, were carried out in order to predict a possible mode of interaction of the best (aza)isoindolinone-type inhibitors with InhA *in vitro*. Then, the work was extended toward evaluations of these compounds against *Mycobacterium tuberculosis* (Mtb) growth and finally some of them were also investigated in respect with their ability to inhibit mycolic acid biosynthesis inside mycobacteria. Although, some azaisoindolinones were able to inhibit InhA activity and Mtb growth *in vitro*, they did not inhibit the mycolic acid biosynthesis inside Mtb.

Introduction

Mycobacterium tuberculosis (Mtb) is the causative agent of tuberculosis, disease that is responsible for the death of 1.5 million people in the world annually (1). Over the years, some strains of mycobacteria have acquired simultaneous resistance to the two most used anti-tubercular drugs: isoniazid (INH) and rifampicin (Multi Drug Resistant strains, MDR). In addition, some strains have even developed resistance not only to the first-line drugs but also to quinolones and a second-line drug (Extremely Drug Resistant strains, XDR). Importantly, the emergence of some strains resistant to all drugs used in anti-tubercular therapeutic regimen (Total Drug Resistant strains, TDR) has also been reported. In this context, tuberculosis represents a serious world health problem. Without effective correct treatments, the concern is that the occurrence of infections caused by MDR-strains will increase and become out of control. Thereby, the need for new anti-tubercular agents with new chemical structure and new mechanism of action appears evident and urgent.

Isoniazid (INH) (Figure 1), one of the most efficient anti-tubercular medicines, is a pro-drug that requires activation by the mycobacterial catalase peroxidase enzyme (KatG) to form, after reaction with the cofactor NAD, the active metabolite (INH-NADH adduct, Figure 1). This adduct exerts its action by inhibiting InhA, an enoyl-ACP-reductase enzyme of Mtb, that is implicated in the mycolic acid biosynthesis, essential constituent of the mycobacterial cell wall. Moreover, it was shown that INH-resistant Mtb strains are frequently correlated to a default of KatG that is unable to activate INH. Direct targeting of InhA appears thus an attractive approach for the discovery of new antibiotic drugs because *i*) InhA is the main target of the confirmed anti-tubercular pro-drug INH, *ii*) enzymes belonging to the Fatty Acid Synthase II (FAS II) system, such as InhA, do not have a human ortholog and *iii)* InhA inhibitor, non KatG dependent, would allow to bypass resistance problems.

Lately, we have been interested in the azaisoindolinone family, designed from the core of the active metabolite of INH (Figure 1), as a promising scaffold for direct InhA inhibition. Our previous work about structure-activity relationship study on azaisoindolinone derivatives has essentially implicated modifications focusing on the hydrocarbon chain (length, position and nature of the linker of the lipophilic chain) and on the tertiary alcohol at C7 position (2, 3). The thiododecyl chain placed in the *meta* position of the phenyl ring was optimal and the free hydroxyl at C7 revealed to be fundamental for InhA inhibition *in vitro* (compound **2a**, Figure 1).

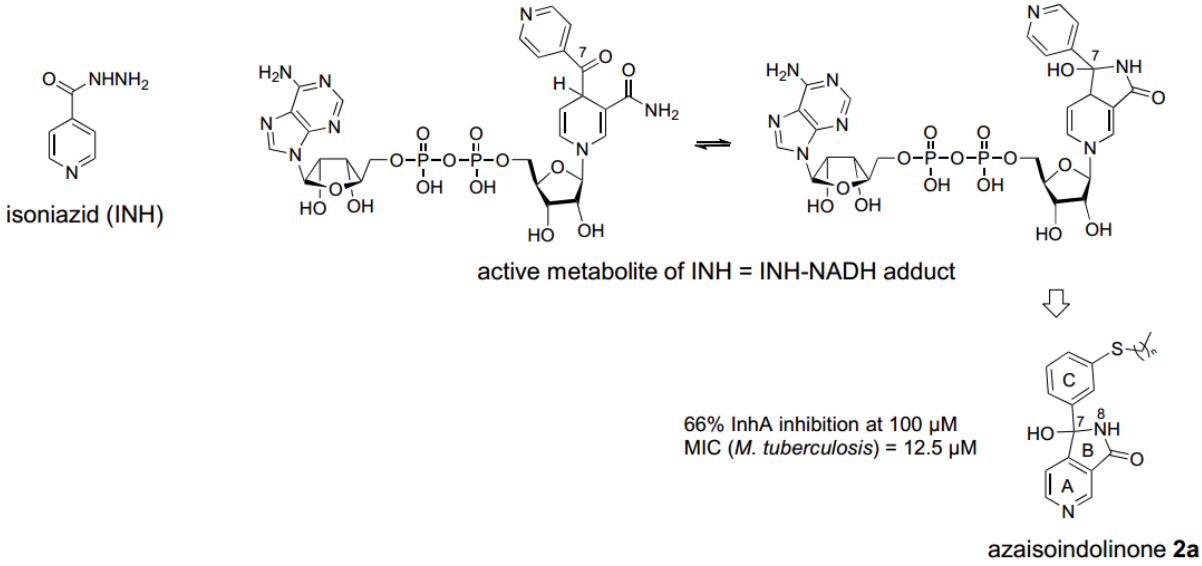

Figure 1. Structures of isoniazid, INH-NADH adduct and azaisoindolinone compound **2a**.

In the continuity with this program, we describe in this paper a study about the structural evolution of azaisoindolinone scaffold **2a**, targeting specific regions of the molecule, as

shown in Figure 2, in order to explore new structure-activity elements and get insights into important structural features to improve inhibitory enzymatic activity. The synthesis of modified azaisoindolinones, their evaluation, as direct inhibitors of the InhA activity *in vitro*, and the simulation of their mode of interaction with InhA by molecular docking experiments were performed. Then the compounds were tested for inhibition of whole cell Mtb growth and an investigation whether the observed inhibition might be correlated to the blockage of mycolic acid biosynthesis was also carried out.

Methods and Materials

Material

All chemicals were obtained from Aldrich or Acros Organics and used without further purification. The melting points were determined on an Electrothermal 9300 capillary melting point apparatus and were not corrected. TLC chromatography (silica gel $F_{254\ nm}$). Infra-red spectra were recorded on a Perkin Elmer Spectrum 100 FT-IR Spectrometer. ^{1}H NMR spectra were recorded on a Bruker spectrometer at 400 and 500 MHz using $CDCl_3$, DMSO-d6 or MeOD-d4 as the solvent. For ^{1}H NMR the residual proton signal of the deuterated solvent was used as an internal reference: $CDCl_3$ δ= 7.29 ppm, DMSO = 2.50 ppm and MeOD = 3.31 ppm. ^{13}C NMR spectra were recorded on a Bruker spectrometer at 100 and 125 MHz. Mass spectra (DCI/NH_3) were obtained on a DSQ Thermo Fisher Scientific. For the MS–ESI a Dionex ultimate 3000 UPLC system with a ABSciex Q TRAP 4500. Flash column chromatography was performed on CombiFlash Companion with silica Redisep columns from 12 g to 80 g. All reagents were obtained from commercial suppliers and were used without further purification. Anhydrous solvents were freshly distilled before use or were obtained from the M.Braun Solvent Purification System (MB-SPS-800). The enzymatic evaluation was performed on a Cary Bio 100.

General protocol for nucleophilic addition of the dodecylthiophenyl moiety

To a solution of 1-bromo-3-dodecylthiobenzene (2 eq) in dry tetrahydrofuran, under argon atmosphere and at -40 °C was added 2.0 M solution of *n*-butyllithium in cyclohexane (2 eq). After addition, the temperature was maintained at -50 °C for 60 min. Then the temperature was decreased at -78 °C and upon this solution was added a solution of the corresponding dione (1 eq) in dry tetrahydrofuran. The reaction mixture was stirred for 30 minutes at -78 °C and was warmed to room temperature for 30 minutes more. The reaction was quenched with a

saturated ammonium chloride solution and the mixture was extracted with ethyl acetate. The organic phases were combined, dried over sodium sulfate and concentrated under vacuum. The residue was chromatographed as indicated in each case to furnish the entitled compound.

(*RS*)-1-[3-(Dodecylsulfanyl)phenyl]-1-hydroxy-1,2-dihydro-3*H*-pyrrolo[3,4-*c*]pyridin-3-one (2a)

Reagents: 1-bromo-3-dodecylthiobenzene (860 mg, 2.4 mmol), dry tetrahydrofuran (10 mL), *n*-butyllithium solution (1.7 mL 2.0 M solution in cyclohexane; 3.4 mmol) and 3,4-pyridinedicarboximide (178 mg, 1.2 mmol). The crude product was purified by flash chromatography (gradient from 100% dichloromethane to 80/20 dichloromethane) to afford a white solid (297 mg, 58%, mixture of *para*/*meta* regioisomers 80/20), mp: 86 °C. TLC R_f: 0.30 (dichloromethane/methanol 95/5). IR (cm^{-1}): 3159, 2917, 2849, 1698, 1614, 1587, 1464, 1347, 1205, 1067, 964, 784, 698. ^{1}H NMR (400 MHz, MeOD) δ (ppm): 8.94 (s, 1H); 8.75 (d, *J* = 5.0 Hz, 1H), 7.55 (s, 1H); 7,46 (d, *J* = 4.6 Hz, 1H); 7.33–7.30 (m, 3H); 2.94 (t, *J* = 7.0 Hz, 2H); 1.63–1.59 (m, 2H); 1.50–1.25 (m, 18H); 0.91 (t, *J* = 6.0 Hz, 3H).^{13}C NMR (100 MHz, MeOD) δ (ppm): 168.3 (C); 159.0 (C); 152.7 (CH); 150.0 (C); 144.5 (CH); 140.0 (C); 138.0 (C); 128.9 (CH); 128.4 (CH); 125.2 (CH); 122.5 (CH); 118.0 (CH); 87.6 (C); 70.1 (CH_2); 32.6 (CH_2); 31.7 (CH_2); 29.4–28.8 (6 x CH_2); 28.4 (CH_2); 22.2 (CH_2); 13.0 (CH_3). MS (ESI) *m/z*: 449.2 [M+Na^+]; 427.3 [M+H^+]. HRMS (ESI): for $C_{25}H_{35}N_2O_2S$ [M+H^+]: calcd: 427.2419; found: 427.2459.

(*RS*)-3-[3-(Dodecylsulfanyl)phenyl]-3-hydroxy-2,3-dihydro-1*H*-isoindol-1-one (2b)

Reagents: 1-bromo-3-dodecylthiobenzene (2.43 g, 6.8 mmol), tetrahydrofuran (5 mL), *n*-butyllithium 2.0 M (3.4 mL solution in cyclohexane; 6.8 mmol) and phtalimide (500 mg, 3.4 mmol). The crude product was purified by flash chromatography (gradient from 100% dichloromethane to 80/20 dichloromethane/methanol) to afford a white solid (696 mg, 48%), mp: 122 °C. TLC R_f: 0.59 (dichloromethane/methanol 90/10). IR (cm^{-1}): 3285, 2918, 2850, 1708, 1665, 1614, 1588, 1466, 1434, 1349, 1192, 1115, 1056, 962, 790, 721, 696. ^{1}H NMR (400 MHz, DMSO-*d6*) δ (ppm): 9.25 (s, 1H); 7.64 (d, *J* = 6.8 Hz, 1H); 7.56-7.46 (m, 2H); 7.40 (s, 1H); 7.33-7.21 (m, 4H); 6.95 (s, 1H); 2.92 (t, *J* = 7.2 Hz, 2H); 1.56–1.49 (m, 2H); 1.45–1.22 (m, 18H); 0.85 (t, *J* = 6.8 Hz, 3H). ^{13}C NMR (100 MHz, DMSO-*d6*) δ (ppm): 168.8 (C); 151.0 (C); 143.5 (C); 137.0 (C); 132.8 (CH); 131.0 (C); 129.5 (CH); 129.4 (CH); 127.5 (CH); 125.2 (CH); 123.2 (CH); 123.1 (CH); 123.0 (CH); 87.6 (C); 32.4 (CH_2); 31.7 (CH_2); 29.5–29.3 (4 x CH_2); 29.2 (CH_2); 29.0 (CH_2); 28.9 (CH_2); 28.6 (CH_2); 22.5 (CH_2); 14.4

(CH_3). MS (DCI/CH_4) *m/z*: 425.2 [M^+]. HRMS (DCI/CH_4): for $C_{26}H_{35}NO_2S$ [M^+]: calcd: 425.2393; found: 425.2389.

(*RS*)-5-Amino-3-[3-(dodecylsulfanyl)phenyl]-3-hydroxy-2-methyl-2,3-dihydro-1*H*-isoindol-1-one (2c)

Reagents: 1-bromo-3-dodecylthiobenzene (1.01 g, 2.8 mmol), dry tetrahydrofuran (5 mL), *n*-butyllithium solution (1.1 mL 2.5 M solution in hexanes; 2.8 mmol) and 4-amino-*N*-methyl-phtalimide (250 mg, 1.4 mmol). The crude product was purified by flash chromatography (gradient from 100% dichloromethane to 80/20 dichloromethane) to afford a white solid (254 mg, 40%), mp: 124 °C. TLC R_f: 0.40 (dichloromethane/methanol 95/5). IR (cm^{-1}): 3459, 3353, 3219, 2921, 2851, 1643, 1605, 1500, 1465, 1422, 1396, 1326, 1194, 1171, 1048, 1031, 970, 742, 701. ^{1}H NMR (400 MHz, DMSO-*d6*) δ (ppm): 7.35-7.18 (m, 4H); 7.01 (d, *J* = 7.6 Hz, 1H); 6.82 (s, 1H); 6.56 (dd, *J* = 2.0 Hz, 8.0 Hz, 1H); 6.35 (d, *J* = 2.0 Hz 1H); 5.77 (s, 2H); 2.92 (t, *J* = 7.2 Hz, 2H); 2.59 (s, 3H) 1.56–1.49 (m, 2H); 1.45–1.22 (m, 18H); 0.86 (t, *J* = 6.8 Hz, 3H). ^{13}C NMR (100 MHz, DMSO-*d6*) δ (ppm): 167.5 (C); 153.4 (C); 152.1 (C); 142.0 (C); 137.3 (C); 129.7 (CH); 127.3 (CH); 125.2 (CH); 124.0 (CH); 123.2 (CH); 117.7 (C); 114.2 (CH); 107.0 (CH); 89.5 (C); 32.3 (CH_2); 31.7 (CH_2); 29.5–29.3 (4 x CH_2); 29.2 (CH_2); 29.0 (CH_2); 28.9 (CH_2); 28.6 (CH_2); 23.7 (CH_3); 22.5 (CH_2); 14.4 (CH_3). MS (DCI/CH_4) *m/z*: 455.3 [M+H^+]. HRMS (DCI/CH_4): for $C_{27}H_{39}N_2O_2S$ [M+H^+]: calcd: 455.2723; found: 455.2732.

(*RS*)-1,2-Dihydroxy-1-[3-(dodecylsulfanyl)phenyl]-1,2-dihydro-3*H*-pyrrolo[3,4-*c*]pyridine-3-one (4a)

Reagents: 1-bromo-3-dodecylthiobenzene (435 mg, 1.2 mmol), dry tetrahydrofuran (3 mL), *n*-butyllithium solution (0.48 mL 2.5 M solution in hexanes, 1.2 mmol) and of 2-hydroxy-2,5-diaza-2*H*-indene-1,3-dione. The crude product was purified by flash chromatography (gradient from 100% dichloromethane to 80/20 dichloromethane) to afford (159 mg, 30% - mixture of *para* and *meta* regioisomers 70/30). TLC R_f: 0.17 (dichloromethane/methanol 95/5). IR (cm^{-1}): 3104, 2922, 2852, 1702, 1616, 1590, 1465, 1433, 1376, 1259, 1203, 1184, 1135, 1109, 1075, 973, 953, 902, 863, 841, 781, 745, 697, 653, 611. MS (ESI) *m/z*: 443.3 [M+H^+]. HRMS (ESI): for $C_{25}H_{35}N_2O_3S$ [M+H^+]: calcd: 443.2367; found: 443.2368

Separation of *p*-4a and *m*-4a by liquid chromatography

Both compounds, *para* and *meta*, were isolated using a HPLC preparative chromatography system (Waters autopurification system), a 2-ethyl-pyridine column 250 x 10.0 mm 5µm and 8% *i*PrOH / 92% CH_2Cl_2 as eluant. Isocatric elution was performed at 6.0 mL/min and absorbance was followed at λ = 254.0 nm. Both regioisomers ***p*-4a** and ***m*-4a** were separated with respective retention times of t_{R1} = 12.4 min and t_{R2} = 13.2 min.

(*RS*)-1,2-Dihydroxy-1-[3-(dodecylsulfanyl)phenyl]-1,2-dihydro-3*H*-pyrrolo[3,4-*c*]pyridine-3-one (*p*-4a)

^{1}H NMR (400 MHz, DMSO-*d6*) δ (ppm): 10.13 (s, 1H), 8.93 (s, 1H); 8.77 (d, *J* = 5.1 Hz, 1H), 7.62 (s, 1H); 7,40 (dd, *J* = 0.9 Hz, 4.6 Hz, 1H); 7.34–7.26 (m, 2H); 7.17–7.11 (m, 1H); 2.94 (t, *J* = 7.2 Hz, 2H); 1.60–1.48 (m, 2H); 1.40–1.16 (m, 18H); 0.87 (t, *J* = 6.3 Hz, 3H). ^{13}C NMR (100 MHz, DMSO-*d6*) δ (ppm): 161.4 (C); 154.4 (C); 153.8 (CH); 144.4 (CH); 139.2 (C); 137.5 (C); 129.7 (CH); 128.1 (CH); 125.7 (CH); 124.8 (C); 123.7 (CH); 118.1 (CH); 89.7 (C); 32.3 (CH_2); 31.8 (CH_2); 29.5-29.4 (4 x CH_2); 29.2 (CH_2); 29.0 (CH_2); 28.9 (CH_2); 28.6 (CH_2); 22.6 (CH_2); 14.4 (CH_3).

(*RS*)-2,3-Dihydroxy-3-(3-(dodecylsulfanyl)phenyl)-2,3-dihydro-1*H*-pyrrolo[3,4-*c*]pyridin-1-one (*m*-4a)

^{1}H NMR (400 MHz, DMSO-*d6*) δ (ppm): 10.25 (s, 1H), 8.78 (d, *J* = 5.1 Hz, 1H); 8.60 (s, 1H), 7.73 (d, *J* = 4.8 Hz, 1H); 7.62 (s, 1H); 7.36–7.25 (m, 3H); 7.18–7.13 (m, 1H); 2.94 (t, *J* = 7.2 Hz, 2H); 1.61–1.48 (m, 2H); 1.42–1.16 (m, 18H); 0.87 (t, *J* = 6.6 Hz, 3H). ^{13}C NMR (100 MHz, DMSO-*d6*) δ (ppm): 160.9 (C); 151.2 (CH); 144.7 (CH); 140.9 (C); 139.6 (C); 137.4 (C); 137.0 (C); 129.7 (CH); 128.1 (CH); 125.7 (CH); 123.7 (CH); 117.0 (CH); 89.8 (C); 32.3 (CH_2); 31.8 (CH_2); 29.5-29.4 (4 x CH_2); 29.2 (CH_2); 29.0 (CH_2); 28.9 (CH_2); 28.6 (CH_2); 22.6 (CH_2); 14.4 (CH_3).

(*RS*)-2,3-Dihydroxy-3-[3-(dodecylsulfanyl)phenyl]-2,3-dihydro-1*H*-isoindol-1-one (4b)

Reagents: 1-bromo-3-dodecylthiobenzene (879 mg, 2.45 mmol), dry tetrahydrofuran (5 mL), *n*-butyllithium (0.98 mL, 2.5 M solution in hexanes; 2.45 mmol) and *N*-hydroxyphtalimide (200 mg, 1.23 mmol). The crude product was purified by flash chromatography (gradient from 80/20 dichloromethane/methanol to 50/50) to afford a white solid (239 mg, 44%), mp: 145 °C. TLC R_f: 0.17 (hexane/ethyl acetate 60/40). IR (cm^{-1}): 3179, 2953, 2920, 2850, 1686, 1617, 1588, 1467, 1432, 1269, 1230, 1202, 1186, 1141, 1095, 1066, 972, 943, 902, 864, 818,

779, 768, 736. ^{1}H NMR (400 MHz, DMSO-*d6*) δ (ppm): 9.89 (s, 1H), 7.69 (d, *J* = 7.2 Hz, 1H); 7.55 (td, *J* = 1.2 Hz, 7.8 Hz, 1H); 7.50 (td, *J* = 1.2 Hz, 7.2 Hz, 1H); 7.33 (s, 1H); 7.31-7.21 (m, 4H); 7.10 (dt, *J* = 1.6 Hz, 7.6 Hz, 1H); 2.91 (t, *J* = 7.6 Hz, 2H); 1.57-1.47 (m, 2H); 1.39-1.16 (m, 18H); 0.85 (t, *J* = 6.4 Hz, 3H). ^{13}C NMR (100 MHz, DMSO-*d6*) δ (ppm): 163.04 (C); 146.8 (C); 140.8 (C); 137.0 (C); 132.8 (CH); 129.7 (CH); 129.4 (CH); 129.1 (C); 127.7 (CH); 125.8 (CH); 123.8 (CH); 123.1 (CH); 122.8 (CH); 90.0 (C); 32.3 (CH_2); 31.7 (CH_2); 29.5 (CH_2); 29.4 (CH_2); 29.3 (CH_2); 29.2 (CH_2); 29.0 (CH_2); 28.9 (CH_2); 28.6 (CH_2); 22.5 (CH_2); 14.4 (CH_3). MS (DCI/CH_4) *m/z*: 464.2 [M+Na^+]. HRMS (DCI/CH_4): for $C_{25}H_{35}NO_3S$.Na [M+Na^+]: calcd: 464.2234; found: 464.2235.

(*RS*)-1-[3-(Dodecylsulfanyl)phenyl]-1-hydroxy-2-methoxy-1,2-dihydro-3*H*-pyrrolo[3,4-*c*] pyridin-3-one (5a)

Reagents: 1-bromo-3-dodecylthiobenzene (200 mg, 0.56 mmol), dry tetrahydrofuran (1.5 mL), *n*-butyllithium solution (0.22 mL 2.5 M solution in hexanes; 0.56 mmol) and 2-methoxy-2,5-diaza-2*H*-indene-1,3-dione (50 mg, 0.28 mmol). The crude product was purified by flash chromatography (gradient from 100% dichloromethane to 90/10 dichloromethane/methanol) to afford an oil (45 mg, 35% - mixture of *para* and *meta* 70/30). A little quantity of the *para* compound was isolated for characterization and biological assay. TLC R_f: 0.36 (dichloromethane/methanol 95/5). IR (cm^{-1}) *for the p/m mixture in a ratio 50/50*: 3249, 2922, 2851, 1713, 1612, 1589, 1459, 1427, 1341, 1255, 1201, 1110, 1075, 1004, 960, 897, 856, 781, 743, 694. *For the pure para compound* ^{1}H NMR (400 MHz, DMSO-*d6*) δ (ppm): 8.98 (s, 1H); 8.80 (d, *J* = 4.8 Hz, 1H) 7.86 (s, 1H); 7.42 (dd, *J* = 1.0 Hz, 5.0 Hz, 1H); 7.35-7.25 (m, 2H); 7.09 (dt, *J* = 1.6 Hz, 6.8 Hz, 1H); 3.85 (s, 3H); 2.92 (t ,*J* = 7.4 Hz, 2H); 1.57-1.48 (m, 2H); 1.37-1.18 (m, 18H); 0.85 (t, *J* = 6.8 Hz, 3H). ^{13}C NMR (100 MHz, DMSO-*d6*) δ (ppm): 161.4 (C); 154.4 (CH); 154.4 (C); 144.8 (CH); 138.8 (C); 137.6 (C); 129.8 (CH); 128.3 (CH); 125.4 (CH); 124.0 (C); 126.6 (CH); 118.0 (CH); 90.2 (C); 65.5 (CH_3); 32.2 (CH_2); 31.7 (CH_2); 29.5 (CH_2); 29.5 (CH_2); 29.4 (CH_2); 29.3 (CH_2); 29.2 (CH_2); 29.0 (CH_2); 28.9 (CH_2); 28.5 (CH_2); 22.5 (CH_2); 14.4 (CH_3). MS (DCI/CH_4) *m/z*: 456.6 [M^+]. HRMS (DCI/CH_4): for $C_{26}H_{36}N_2O_3S$ [M^+]: calcd: 456.2452; found: 456.2447.

(*RS*)-3-[3-(Dodecylsulfanyl)phenyl]-3-hydroxy-2-methoxy-2,3-dihydro-1*H*-isoindol-1-one (5b)

Reagents: 1-bromo-3-dodecylthiobenzene (660 mg, 1.8 mmol), dry tetrahydrofuran (5 mL), *n*-butyllithium solution (0.74 mL 2.5 M solution in hexanes; 1.8 mmol) and 2-methoxy-2*H*-isoindole-1,3-dione (164 mg, 0.92 mmol). The crude product was purified by flash chromatography (gradient from 80/20 hexane/ethyl acetate to 60/40) to afford a white solid (101 mg, 24%), mp: 97 °C. TLC R_f: 0.29 (hexane/ethyl acetate 70/30). IR (cm^{-1}): 3223, 2917, 2849, 1694, 1614, 1588, 1467, 1435, 1357, 1205, 1115, 1093, 1061, 1023, 1005, 963, 953, 901, 884, 857, 789, 766, 738, 719, 691. ^{1}H NMR (400 MHz, DMSO-*d6*) δ (ppm): 7.75 (d, *J* = 8.8 Hz, 1H); 7.66-7.50 (m, 3H); 7.36-7.20 (m , 3H); 7.07 (dt, *J* = 1.8 Hz, 7.2 Hz); 3.85 (s, 1H); 2.90 (t, *J* = 7.2 Hz, 2H); 1.55-1.46 (m, 2H); 1.35-1.18 (m, 18H); 0.85 (t, *J* = 6.6 Hz, 3H). ^{13}C NMR (100 MHz, DMSO-*d6*) δ (ppm): 163.1 (C); 146.8 (C); 140.4 (C); 137.2 (C); 133.7 (CH); 130.0 (CH); 129.6 (CH); 128.2 (C); 127.8 (CH); 125.5 (CH); 123.6 (CH); 123.2 (2 x CH); 90.5 (C); 65.3 (CH_3); 32.3 (CH_2); 31.7 (CH_2); 29.5 (CH_2); 29.5 (CH_2); 29.4 (CH_2); 29.3 (CH_2); 29.2 (CH_2); 29.0 (CH_2); 28.9 (CH_2); 28.5 (CH_2); 22.5 (CH_2); 14.4 (CH_3). MS (DCI/CH_4) *m/z*: 455.2 [M^+]. HRMS (DCI/CH_4): for $C_{27}H_{37}NO_3S$ [M^+]: calcd: 455.2493; found: 455.2494.

(*RS*)-1-[3-(Dodecylsulfonyl)phenyl]-1-hydroxy-1,2-dihydro-3*H*-pyrrolo[3,4-c]pyridin-3-one 5-oxide (3)

To a solution of (*RS*)-1-[3-(dodecylsulfanyl)phenyl]-1-hydroxy-1,2-dihydro 3*H*-pyrrolo[3,4-*c*]pyridin-3-one (63 mg, 0.15 mmol, 1 eq) in dichloromethane (5 mL) was added at room temperature 3-chloro-peroxobenzoic acid (*m*CPBA). The mixture was stirred for 3 hours then 10 mL of brine were added and the entitled product was extracted with dichloromethane (3 x 10 mL). The organic phases were combined, dried over sodium sulfate and concentrated under vacuum. The residue was purified by flash chromatography (gradient from 100% dichloromethane to 80/20 dichloromethane) to furnish a white solid (51 mg, 72%) mp: 175 °C. TLC R_f: 0.21 (dichloromethane/methanol 95/5). IR (cm^{-1}): 3117, 3036, 2957, 2922, 2852, 2806, 1708, 1445, 1396, 1323, 1301, 1220, 1136, 1095, 1058, 1022, 864. ^{1}H NMR (400 MHz, DMSO-*d6*) δ (ppm): 9.84 (s, 1H); 8.45 (s, 1H); 8.30 (dd, *J* = 1.6 Hz, 6.4 Hz, 1H); 8.05 (t, *J* = 1.6 Hz); 7.89 (d, *J* = 8.0 Hz, 1H); 7.83 (d, *J* = 8.4 Hz, 1H); 7.67 (t, *J* = 7.8 Hz, 1H); 7.52 (s, 1H); 7.42 (d, *J* = 6.8 Hz, 1H); 3.30 (t, *J* = 8.4 Hz, 2H); 1.57-1.47 (m, 2H); 1.32-1.15 (m, 18H); 0.85 (t, *J* = 6.8 Hz, 3H). ^{13}C NMR (100 MHz, DMSO-*d6*) δ (ppm): 165.2 (C); 145.5 (C); 143.0 (CH); 142.3 (C); 140.0 (C); 134.1 (CH); 131.5 (CH); 130.9 (C); 130.3 (CH); 128.3

(CH); 125.1 (CH); 121.1 (CH); 87.0 (C); 54.9 (CH_2); 31.7 (CH_2); 29.4 (2 x CH_2); 29.3 (CH_2); 29.1 (2 x CH_2); 28.8 (CH_2); 27.8 (CH_2); 22.5 (CH_2); 14.4 (CH_3). MS (ESI) *m/z*: 475.2 [M+H^+]. HRMS (ESI): for $C_{25}H_{35}N_2O_5S$: calcd: 475.2267; found: 475.2269.

General protocol for the synthesis of pyridazinone containing derivatives

Corresponding *N*-methoxyisoindolinone type compound (1 eq), ethanol (10 mL), and hydrazine hydrate (15 eq) were added into a round-bottom flask equipped with a condenser. A nitrogen balloon was attached to the top of the condenser. After refluxing overnight, the reaction was cooled to room temperature. An off-white solid precipitated out of the solution. After cooling to 0 °C, water was added slowly and the compound was extracted with dichloromethane (3 x 10 mL). The residue was purified by flash chromatography to furnish the entitled compound.

1-[3-(Dodecylsulfanyl)phenyl]-pyrido[3,4-*d*]pyridazin-4(3*H*)-one (6a)

Reagents: (*RS*)-1-[*3*-(dodecylthio)phenyl]-1-hydroxy-2-methoxy-1,2-dihydro-3*H*-pyrrolo[3,4-c]pyridin-3-one (**5a)** and its *meta* regioisomer (in a ratio *para*/*meta* 60/40, 64 mg, 0.14 mmol), ethanol (10 mL) and hydrazine hydrate (0.1 mL, 2.09 mmol).

The crude product was purified by flash chromatography (gradient from 100% dichloromethane to 90/10 dichloromethane/methanol) to afford a yellow solid (57 mg, 96% - mixture of *para* and *meta* compounds 60/40). The *para* compound was isolated for characterization and biological activity evaluation. TLC R_f: 0.56 for the *para* compound and 0.66 for the *meta* compound (dichloromethane/methanol 95/5). IR (cm^{-1}) *for the mixture of para/meta 60/40*: 2918, 2850, 1707, 1666, 1599, 1566, 1466, 1410, 1333, 1318, 1277, 1217, 1176, 1134, 1101, 1082, 1044, 998, 885, 853, 806, 783, 701, 681, 662, 610, 557. *For the pure para compound* ^{1}H NMR (400 MHz, DMSO-*d6*) δ (ppm): 13.19 (s, 1H); 9.52 (s, 1H); 9.01 (d, *J* = 5.2 Hz, 1H); 7.54 (d, *J* = 5.6 Hz, 1H); 7.53-7.43 (m, 3H); 7.42-7.37 (m, 1H); 3.01 (t, *J* = 7.2 Hz, 2H); 1.65-1.55 (m, 2H); 1.44-1.15 (m, 18H); 0.85 (t, *J* = 6.8 Hz, 3H). ^{13}C NMR (100 MHz, DMSO-*d6*) δ (ppm): 158.8 (C); 153.5 (CH); 149.9 (CH); 145.2 (C); 138.0 (C); 135.1 (C); 134.3 (C); 129.7 (CH); 128.9 (CH); 128.3 (CH); 126.7 (CH); 122.3 (C); 119.1 (CH); 32.2 (CH_2); 31.7 (CH_2); 29.5 (CH_2); 29.4 (CH_2); 29.4 (CH_2); 29.3 (CH_2); 29.1 (CH_2); 28.9 (CH_2); 28.9 (CH_2); 28.5 (CH_2); 22.5 (CH_2); 14.4 (CH_3). MS (ESI) *m/z*: 424.2 [M+H^+]. HRMS (ESI): for $C_{25}H_{34}N_3OS$ [M+H^+]: calcd: 424.2421; found: 424.2423.

4-[3-(Dodecylsulfanyl)phenyl]phthalazin-1(2*H*)-one (6b)

Reagents: (*RS*)-3-[3-(Dodecylsulfanyl)phenyl]-3-hydroxy-2-methoxy-2,3-dihydro-1*H*-isoindol-1-one (**5b**) (57 mg, 0.14 mmol), ethanol (10 mL) and hydrazine hydrate (0.11 mL, 2.13 mmol).

The crude product was purified by flash chromatography (isocratic 80/20 hexane/ethyl) to afford a white solid (15 mg, 26%). TLC R_f: 0.72 (dichloromethane/methanol 95/5). IR (cm^{-1}): 2914, 2849, 1683, 1567, 1339, 1223, 1155, 995, 896, 782, 721, 697, 685. ^{1}H NMR (500 MHz, $CDCl_3$) δ (ppm): 12.86 (s, 1H); 8.39-8.31 (m, 1H); 7.90 (t, *J* = 5.2 Hz, 2H); 7.68-7.63 (m, 1H); 7.51-7.44 (m, 3H); 7.38 (d, *J* = 7.2 Hz, 1H); 3.01 (t, *J* = 7.2 Hz, 2H); 1.61 (m, 2H); 1.42-1.35 (m, 2H); 1.30-1.15 (m, 16H); 0.84 (t, *J* = 6.8 Hz, 3H). ^{13}C NMR (125 MHz, DMSO-*d6*) δ (ppm): 159.7 (C); 146.5 (C); 137.7 (C); 136.3 (C); 134.1 (CH); 132.2 (CH); 129.6 (CH); 129.4 (C); 128.7 (CH); 128.6 (CH); 128.3 (C); 126.9 (CH); 126.8 (CH); 126.6 (CH); 32.2 (CH_2); 31.7 (CH_2); 29.5 (3 x CH_2); 29.4 (CH_2); 29.3 (CH_2); 29.1 (CH_2); 28.9 (CH_2); 28.5 (CH_2); 22.5 (CH_2); 14.4 (CH_3). MS (DCI/CH_4) *m/z*: 423.6 [M+H$^+$]. HRMS (DCI/CH_4): for $C_{26}H_{34}N_2OS$ [M+H$^+$]: calcd: 423.2480; found: 423.2470.

General protocol for addition of ethynyl-TMS group

To a solution of ethynyl-trimethylsilane (2 eq) in dry tetrahydrofuran, under argon atmosphere and at -40 °C was added *n*-butyllithium 2.5M solution (2 eq). After addition, the temperature was maintained at -50 °C for 60 min. Then the temperature was decreased at -78 °C and upon this solution was added a solution of the corresponding (aza)-isoindolinone starting material (1 eq) in dry tetrahydrofuran. The reaction mixture was stirred for 30 minutes at -78 °C and was warmed to room temperature for 30 minutes more. The reaction was quenched with a saturated ammonium chloride solution and the product was extracted with ethyl acetate. The organic phases were combined, dried over sodium sulfate and concentrated under vacuum. The residue was purified by flash chromatography to furnish the entitled compound.

(*RS*)-1-Hydroxy-1-[2-(trimethylsilyl)ethynyl]-1,2-dihydro-3*H*-pyrrolo[3,4-*c*]pyridine-3-one (7a)

Reagents: ethynyltrimethylsilane (663 mg, 0.95 mL, 6.65 mmol), dry tetrahydrofuran (10 mL), *n*-butyllithium solution (2.7 mL 2.5M solution in hexanes; 6.65 mmol) and 3,4-pyridinedicarboximide (500 mg, 3.37 mmol). The crude product was purified by flash chromatography (gradient from 100% dichloromethane to 90/10 dichloromethane/methanol) to afford a white solid (407 mg, 49%), mp: 170 °C. TLC R_f: 0.31 (dichloromethane/methanol

90/10). IR (cm^{-1}): 3203, 3067, 2958, 2897, 2735, 1710, 1690, 1616, 1556, 1488, 1459, 1436, 1381, 1338, 1286, 1213, 1168, 1125, 1049, 837, 798, 759. ^{1}H NMR (400 MHz, DMSO-*d6*) δ (ppm): 9.70 (s, 1H); 8.89-8.86 (m, 2H); 7.70 (dd, *J* = 1.2 Hz, 5.2 Hz, 1H); 7.39 (s, 1H); 0.15 (s, 9H). ^{13}C NMR (100 MHz, DMSO-d5) δ (ppm): 166.6 (C); 156.2 (C); 154.1 (CH); 145.1 (CH); 125.9 (C); 118.1 (CH); 103.0 (C); 88.5 (C); 79.3 (C); 0.0 (3 x CH_3). MS (DCI/CH_4) *m/z*: 247.1 [M+H^+]. HRMS (DCI/CH_4): for $C_{12}H_{14}N_2O_2Si$ [M+H^+]: calcd: 247.0905; found: 247.0903.

(*RS*)-3-Hydroxy-3-[2-(trimethylsilyl)ethynyl]-2,3-dihydro-1*H*-isoindol-1-one (7b)

Reagents: ethynyltrimethylsilane (133 mg, 0.19 mL, 1.36 mmol), dry tetrahydrofuran (2.5 mL), *n*-butyllithium solution (0.68 mL 2.5 M solution in hexanes, 1.36 mmol) and phtalimide (100 mg, 0.68 mmol).

The crude product was purified by flash chromatography (gradient from 100% dichloromethane to 85/15 dichloromethane/methanol) to afford a white solid (97 mg, 58%), mp: 168 °C. TLC R_f: 0.26 (dichloromethane/methanol 95/5). IR (cm^{-1}): 3310, 3219, 2959, 2900, 2799, 1708, 1689, 1615, 1471, 1425, 1347, 1321, 1272, 1249, 1210, 1161, 1128, 1094, 1061, 1047, 1020, 839, 756, 694. ^{1}H NMR (400 MHz, $CDCl_3$) δ (ppm): 7.80 (d, *J* = 7.6 Hz, 1H); 7.74-7.66 (m, 2H); 7.58 (t, *J* = 7.2 Hz, 1H); 0.20 (s, 9H). ^{13}C NMR (100 MHz, $CDCl_3$) δ (ppm): 169.3 (C); 146.9 (C); 133.5 (CH); 130.4 (CH); 129.3 (C); 123.8 (CH); 122.8 (CH); 100.5 (C); 90.2 (C); 53.4 (C); 0.46 (3 x CH_3). MS (DCI/CH_4) *m/z*: 246.1 [M+H^+]. HRMS (DCI/CH_4): for $C_{13}H_{15}NO_2Si$ [M+H+]: calcd: 246.0947; found: 246.0950.

General protocol for the Huisgen type cycloaddition reaction

To a solution of the corresponding (trimethylsilyl)ethynylisoindolinone intermediate (1.0 eq) and alkyl azide with a defined number of carbons (1.1 eq) in methanol were added copper(II) sulfate pentahydrate (0.2 eq), sodium ascorbate (0.4 eq) and finally tetrabutylammonium fluoride (TBAF) solution (1.0 eq) to start the click chemistry reaction. The mixture was stirred for 16 hours and then was concentrated under vacuum and directly purified by flash chromatography to furnish the entitled compound.

For starting compounds with a pyridine moiety, an additional washing step with a saturated solution of ethylenediaminetetraacetic acid (EDTA) was needed to remove copper.

(*RS*)-1-Hydroxy-1-(1-octyl-1*H*-1,2,3-triazol-4-yl)-1-hydroxy-1,2-dihydro-3*H*-pyrrolo[3,4-*c*]pyridin-3-one (8a)

Reagents: (*RS*)-3-hydroxy-3-[2-(trimethylsilyl)ethynyl]-2,3-dihydro-1*H*-isoindol-1-one (65 mg, 0.32 mmol), 1-octyl-azide (55 mg, 0.36 mmol), methanol (10 mL), copper(II) sulfate pentahydrate (16 mg, 0.04 mmol), sodium ascorbate (26 mg, 0.13 mmol, 0.4 eq) and tetrabutylammonium fluoride solution (0.32 mL of a 1.0 M solution in tetrahydrofuran, 0.32 mmol). The crude product was purified by flash chromatography (gradient from 100% dichloromethane to 90/10 dichloromethane/methanol) to afford (86 mg, 82%), mp: 175 °C. TLC R_f: 0.42 (dichloromethane/methanol 90/10). IR (cm^{-1}): 3120, 3072, 2946, 2917, 2849, 2776, 1725, 1616, 1492, 1464, 1436, 1395, 1377, 1345, 1288, 1260, 1230, 1156, 1141, 1081, 1052, 1034, 929, 839, 795, 734. ^{1}H NMR (400 MHz, DMSO-*d6*) δ (ppm): 9.53 (s, 1H); 8.87 (s, 1H); 8.78 (d, *J* = 5.2 Hz, 1H); 8.25 (s, 1H); 7.53 (dd, *J*= 1.0 Hz, 5.0 Hz, 1H); 7.21 (s, 1H); 4.34 (t, *J* = 7 Hz, 2H); 1.84-1.75 (m, 2H); 1.30-1.17 (m, 10H); 0.85 (t, *J* = 6.8 Hz, 3H). ^{13}C NMR (100 MHz, DMSO-*d6*) δ (ppm): 167.2 (C); 157.6 (C); 153.4 (CH); 147.9 (C); 144.9 (CH); 126.8 (C); 123.4 (CH); 118.6 (CH); 84.1 (C); 49.9 (CH_2); 31.6 (CH_2); 30.1 (CH_2); 29.0 (CH_2); 28.8 (CH_2); 26.3 (CH_2); 22.5 (CH_2); 14.4 (CH_3). MS (DCI/CH_4) *m/z*: 330.2 [M+H^+]. HRMS (DCI/CH_4): for $C_{17}H_{24}N_5O_2$ [M+H^+]: calcd: 330.1941; found: 330.1930.

(*RS*)-1-(1-Decyl-1*H*-1,2,3-triazol-4-yl)-1-hydroxy1-1,2-dihydro-3*H*-pyrrolo [3,4*c*]pyridin-3-one (9a)

Reagents: (*RS*)-3-hydroxy-3-[2-(trimethylsilyl)ethynyl]-2,3-dihydro-1*H*-isoindol-1-one (70 mg, 0.32 mmol), 1-decyl-azide (65 mg, 0.36 mmol), methanol (10 mL), copper(II) sulfate pentahydrate (16 mg, 0.04 mmol), sodium ascorbate (26 mg, 0.13 mmol) and tetrabutylammonium fluoride solution (0.32 mL of a 1.0 M solution in tetrahydrofuran, 0.32 mmol).

The crude product was purified by flash chromatography (gradient from 100% dichloromethane to 90/10 dichloromethane/methanol) to afford a yellow solid (107 mg, 94%), mp: 168 °C. TLC R_f: 0.44 (dichloromethane/methanol 90/10). IR (cm^{-1}): 3120, 3072, 2916, 2849, 1725, 1615, 1492, 1462, 1435, 1345, 1284, 1156, 1140, 1082, 1052, 1034, 930, 839, 8223, 796, 758, 736. ^{1}H NMR (400 MHz, DMSO-*d6*) δ (ppm): 9.53 (s, 1H); 8.87 (s, 1H); 8.78 (d, *J* = 5.2 Hz, 1H); 8.25 (s, 1H); 7.53 (dd, *J*= 1.0 Hz, 5.0 Hz, 1H); 7.21 (s, 1H); 4.34 (t, *J* = 7 Hz, 2H); 1.84-1.75 (m, 2H); 1.30-1.17 (m, 14H); 0.85 (t, *J* = 6.8 Hz, 3H). ^{13}C NMR (100 MHz, DMSO-*d6*) δ (ppm): 167.2 (C); 157.6 (C); 153.4 (CH); 147.9 (C); 144.9 (CH); 126.8 (C); 123.4 (CH); 118.6 (CH); 84.1 (C); 49.9 (CH_2); 31.6 (CH_2); 30.1 (CH_2); 29.4 (CH_2); 29.3

(CH_2); 29.1 (CH_2); 28.8 (CH_2); 26.3 (CH_2); 22.5 (CH_2); 14.4 (CH_3). MS (DCI/CH_4) *m/z*: 358.2 [M+H^+]. HRMS (DCI/CH_4): for $C_{19}H_{28}N_5O_2$ [M+H^+]: calcd: 358.2243; found: 358.2243.

(*RS*)-1-(1-dodecyl-1*H*-1,2,3-triazol-4-yl)-1-hydroxy1-1,2-dihydro-3*H*-pyrrolo[3,4-*c*]pyridin-3-one (10a)

Reagents: (*RS*)-3-hydroxy-3-[2-(trimethylsilyl)ethynyl]-2,3-dihydro-1*H*-isoindol-1-one (80 mg, 0.32 mmol), 1-dodecyl-azide (76 mg, 0.36 mmol), methanol (10 mL), copper(II) sulfate pentahydrate (16 mg, 0.04 mmol), sodium ascorbate (26 mg, 0.13 mmol) and tetrabutylammonium fluoride solution (0.32 mL of a 1.0 M solution in tetrahydrofuran, 0.32 mmol).

The crude product was purified by flash chromatography (gradient from 100% dichloromethane to 90/10 dichloromethane/methanol) to afford a yellow solid (107 mg, 87%), mp: 168 °C. TLC R_f: 0.46 (dichloromethane/methanol 90/10). IR (cm^{-1}): 3120, 3073, 2917, 2849, 1726, 1615, 1463, 1436, 1344, 1285, 1260, 1231, 1216, 1155, 1141, 1081, 1052, 1034, 929, 821, 796, 759, 734, 661. ^{1}H NMR (400 MHz, DMSO-*d6*) δ (ppm): 9.52 (s, 1H); 8.87 (s, 1H); 8.78 (d, *J* = 5.2 Hz, 1H); 8.25 (s, 1H); 7.53 (dd, *J*= 1.0 Hz, 5.0 Hz, 1H); 7.20 (s, 1H); 4.33 (t, *J* = 7 Hz, 2H); 1.84-1.75 (m, 2H); 1.30-1.17 (m, 18H); 0.85 (t, *J* = 6.8 Hz, 3H). ^{13}C NMR (100 MHz, DMSO-*d6*) δ (ppm): 167.2 (C); 157.6 (C); 153.4 (CH); 147.9 (C); 144.9 (CH); 126.8 (C); 123.4 (CH); 118.6 (CH); 84.1 (C); 49.9 (CH_2); 31.6 (CH_2); 30.1 (CH_2); 29.5 (CH_2); 29.4 (CH_2); 29.4 (CH_2); 29.3 (CH_2); 29.1 (CH_2); 28.8 (CH_2); 26.3 (CH_2); 22.5 (CH_2); 14.4 (CH_3). MS (DCI/CH_4) *m/z*: 386.2 [M+H^+]. HRMS (DCI/CH_4): for $C_{21}H_{32}N_5O_2$ [M+H^+]: calcd: 386.2552; found: 386.2556.

(*RS*)-3-Hydroxy-3-(1-octyl-1*H*-1,2,3-triazol-4-yl)-2,3-dihydro-1*H*-isoindol-1-one (8b)

Reagents: (*RS*)-1-hydroxy-1-[2-(trimethylsilyl)ethynyl]-1,2-dihydro-3*H*-pyrrolo[3,4-*c*]pyridin-3-one (52 mg, 0.21 mmol), 1-octyl-azide (36 mg, 0.23 mmol), methanol (5 mL), copper(II) sulfate pentahydrate (10 mg, 0.04 mmol), sodium ascorbate (17 mg, 0.08 mmol) and tetrabutylammonium fluoride solution (0.21 mL of a 1.0 M solution in tetrahydrofuran, 0.21 mmol). The crude product was purified by flash chromatography (gradient from 100% dichloromethane to 90/10 dichloromethane/methanol) to afford a yellow solid (28 mg, 40%), mp: 132 °C. TLC R_f: 0.54 (dichloromethane/methanol 90/10). IR (cm^{-1}): 3289, 3174, 3129, 2923, 2853, 1683, 1614, 1468, 1424, 1378, 1353, 1316, 1266, 1222, 1199, 1179, 1143, 1081, 1061, 1048, 1025, 918, 855, 762, 737, 718. ^{1}H NMR (400 MHz, DMSO-*d6*) δ (ppm): 9.25 (s,

1H); 8.18 (s, 1H); 7.65-7.45 (m, 4H); 6.91 (s, 1H); 4.32 (t, *J* = 7.0 Hz, 2H); 1.84 (m, 2H); 1.30-1.20 (m, 10H); 0.85 (t, *J* = 6.8 Hz, 3H). ^{13}C NMR (100 MHz, DMSO-*d6*) δ (ppm): 168.5 (C); 149.9 (C); 149.1 (C); 132.7 (CH); 131.3 (C); 129.6 (CH); 123.5 (CH); 123.1 (CH); 122.8 (CH); 84.2 (C); 49.8 (CH_2); 31.6 (CH_2); 30.2 (CH_2); 29.0 (CH_2); 28.8 (CH_2); 26.3 (CH_2); 22.5 (CH_2); 14.4 (CH_3). MS (DCI/CH_4) *m/z*: 329.2 [M+H$^+$]. HRMS (DCI/CH_4): for $C_{18}H_{25}N_4O_2$ [M+H$^+$]: calcd: 329.1986; found: 329.1978.

(*RS*)- 3-(1-Decyl-1*H*-1,2,3-triazol-4-yl)- 3-hydroxy-2,3-dihydro-1*H*-isoindol-1-one (9b)

Reagents: (*RS*)-1-hydroxy-1-[2-(trimethylsilyl)ethynyl]-1,2-dihydro-3*H*-pyrrolo[3,4-*c*]pyridin-3-one (100 mg, 0.41 mmol), 1-decyl-azide (75 mg, 0.45 mmol), methanol (10 mL), copper(II) sulfate pentahydrate (20 mg, 0.08 mmol), sodium ascorbate (32 mg, 0.16 mmol) and tetrabutylammonium fluoride solution (0.41 mL of a 1.0 M solution in tetrahydrofuran, 0.41 mmol). The crude product was purified by flash chromatography (gradient from 100% dichloromethane to 90/10 dichloromethane/methanol) to afford a yellow solid (102 mg, 70%), mp: 145 °C. TLC R_f: 0.43 (dichloromethane/methanol 90/10). IR (cm^{-1}): 3292, 3179, 3130, 2920, 2851, 1684, 1614, 1470, 1424, 1352, 1315, 1266, 1222, 1190, 1143, 1081, 1048, 1026, 917, 880, 854, 803, 761, 737, 720. ^{1}H NMR (400 MHz, DMSO-*d6*) δ (ppm): 9.25 (s, 1H); 8.18 (s, 1H); 7.65-7.45 (m, 4H); 6.91 (s, 1H); 4.32 (t, *J* = 7.0 Hz, 2H); 1.80 (m, 2H); 1.31-1.18 (m, 14H); 0.85 (t, *J* = 6.8 Hz, 3H). ^{13}C NMR (100 MHz, DMSO-*d6*) δ (ppm): 168.5 (C); 149.9 (C); 149.1 (C); 132.7 (CH); 131.3 (C); 129.6 (CH); 123.5 (CH); 123.1 (CH); 122.8 (CH); 84.2 (C); 49.8 (CH_2); 31.7 (CH_2); 30.2 (CH_2); 29.4 (CH_2); 29.3 (CH_2); 29.1 (CH_2); 28.8 (CH_2); 26.3 (CH_2); 22.5 (CH_2); 14.4 (CH_3). MS (DCI/CH_4) *m/z*: 357.2 [M+H$^+$]. HRMS (DCI/CH_4): for $C_{20}H_{28}N_4O_2$ [M+H$^+$]: calcd: 357.2304; found: 357.2291.

(*RS*)-3-(1-Dodecyl-1*H*-1,2,3-triazol-4-yl)- 3-hydroxy-2,3-dihydro-1*H*-isoindol-1-one (10b)

Reagents: (*RS*)-1-hydroxy-1-[2-(trimethylsilyl)ethynyl]-1,2-dihydro-3*H*-pyrrolo[3,4-*c*]pyridin-3-one (100 mg, 0.41 mmol), 1-dodecyl-azide (95 mg, 0.45 mmol), methanol (10 mL), copper(II) sulfate pentahydrate (20 mg, 0.08 mmol), sodium ascorbate (32 mg, 0.16 mmol) and tetrabutylammonium fluoride solution (0.41 mL of a 1.0 M solution in tetrahydrofuran, 0.41 mmol).

The crude product was purified by flash chromatography (gradient from 100% dichloromethane to 90/10 dichloromethane/methanol) to afford a yellow solid (85 mg, 54%), mp: 145 °C. TLC R_f: 0.41 (dichloromethane/methanol 90/10). IR (cm^{-1}): 3292, 3175, 3131 2955, 2919, 2851, 1685, 1614, 1470, 1425, 1377, 1351, 1315, 1265, 1221, 1186, 1143, 1081,

1062, 1048, 916, 880, 855, 803, 761, 737, 721. ^{1}H NMR (400 MHz, DMSO-*d6*) δ (ppm): 9.25 (s, 1H); 8.18 (s, 1H); 7.65-7.45 (m, 4H); 6.91 (s, 1H); 4.32 (t, *J* = 7.0 Hz, 2H); 1.85-1.75 (m, 2H); 1.31-1.18 (m, 18H); 0.85 (t, *J* = 6.8 Hz, 3H). ^{13}C NMR (100 MHz, DMSO-*d6*) δ (ppm): 168.5 (C); 149.9 (C); 149.1 (C); 132.7 (CH); 131.3 (C); 129.6 (CH); 123.5 (CH); 123.1 (CH); 122.8 (CH); 84.2 (C); 49.8 (CH_2); 31.7 (CH_2); 30.2 (CH_2); 29.5 (CH_2); 29.4 (CH_2); 29.4 (CH_2); 29.3 (CH_2); 29.2 (CH_2); 28.8 (CH_2); 26.3 (CH_2); 22.5 (CH_2); 14.4 (CH_3). MS (DCI/CH_4) *m/z*: 385.2 [M+H$^+$]. HRMS (DCI/CH_4): for $C_{22}H_{33}N_4O_2$ [M+H$^+$]: calcd: 385.2598; found: 385.2604.

Biology

InhA expression and purification

The production and purification of the InhA-6xHis protein from a protease-deficient strain of *E. coli* BL21(DE3) transformed with the pHAT5/*inhA* plasmid were performed as followed. 1 mL of the bacteria was grown in 100 mL of LB medium containing ampicillin (100 mg/mL) at 37 °C. After 4 h, the solution was re-diluted in 1 L of the same medium and re-grown at 37 °C. When the proper concentration (OD_{595} = 0.6-0.8) was reached, protein expression was induced by overnight incubation with 1 mM isopropyl-β-D-galactopyranoside (IPTG) at 20 °C. Cells were harvested by centrifugation at 6,000 g for 30 min at 4 °C. The dry pellet may be kept at -80°C for several months. Thawed cells (1.5 g) were sonicated in 20 mL lysis buffer (300 mM NaCl, 10 mM imidazole, 50 mM sodium phosphate buffer, pH 8.0). After centrifugation at 10,000 g for 45 min at 4 °C, the supernatant was applied onto a nickel-chelated Hi-Trap HP 1 mL column (GE Healthcare) previously equilibrated with the binding buffer (50 mM NaCl, 10 mM imidazole, 50 mM sodium phosphate buffer, pH 8,0). First, the unbound proteins were washed out with 10 column volume of binding buffer, and then a higher imidazole concentration (25 mM) allowed the elution of non-specifically bound proteins. The His_6-tagged InhA protein was eluted with an imidazole gradient from 25 mM to 300 mM over a range of 20 column volume. Fractions containing the target protein were pooled, concentrated to 2.0 mL and loaded on a HiLoad 16/60 Superdex 200 column (GE Healthcare) equilibrated with 150 mM NaCl, 30 mM PIPES, pH 6.8. Samples were analyzed using SDS-PAGE and Coomassie blue staining and then stored at 4 °C for short term storage 80 °C with 20% glycerol for long-term storage.

InhA activity inhibition

Triclosan and NADH were obtained from Sigma-Aldrich. Stock solutions of all compounds were prepared in DMSO such that the final concentration of this co-solvent was constant at 5% v/v in a final volume of 1 mL for all kinetic reactions. Kinetic assays were performed using *trans*-2-dodecenoyl-coenzyme A (DDCoA) and wild type InhA as previously described. Briefly, pre-incubation reactions were performed in an aqueous buffer (30 mM PIPES and 150 mM NaCl pH 6.8) containing additionally 100 nM InhA, 250 µM cofactor (NADH) and the tested compound (50 µM or 10 µM). After 5 min of pre-incubation at 25 °C, addition of 50 µM DDCoA initiated the reaction which was followed at 340 nm (oxidation of NADH). The inhibitory activity of each derivative was expressed as the percentage of inhibition of InhA activity (initial velocity of the reaction) with respect to the control reaction without inhibitor. Triclosan was used as a positive control. All activity assays were performed in triplicate.

Mycobacterium growth inhibition

H37Rv was used as the reference strain. The strains were grown at 37°C in Middlebrook 7H9 broth (Difco), supplemented with 0.05% Tween 80, or on solid Middlebrook 7H11 medium (Difco) supplemented with oleic acid-albumin-dextrose-catalase (OADC). MICs for the new compounds were determined by means of the micro-broth dilution method. Dilutions of *M. tuberculosis* wild-type (about 10^5-10^6 cfu/ml) were streaked onto 7H11 solid medium containing a range of drug concentrations (0.25 µg/mL to 40 µg/mL). Plates were incubated at 37 °C for about 21 days and the growth was visually evaluated. The lowest drug dilution at which visible growth failed to occur was taken as the MIC value. Results were expressed as the average of at least three independent determinations.

Acid mycolic biosynthesis inhibition

INH, **2a** and ***m*-4a** were added to broth cultures of *M. tuberculosis* H37Rv during the exponential growth phase at their MIC (1 µM, 25 µM and 12.5 µM respectively). The cultures were then incubated at 37 °C for 5 h before the addition of [1-^{14}C]acetate (1 µCi, 17 µM) to follow the biosynthesis of lipid products. Cells were incubated for 18 h and then harvested. Fatty and mycolic acids were released from whole bacteria through saponification by incubating the latter with a mixture of 40% KOH (w/v) in methoxyethanol (1/7) for 6 h at 100 °C. After acidification by addition of 20% H_2SO_4, lipids including mycolic acids were extracted with diethyl ether. The crude fatty acids were methylated and methyl ester

derivatives were analyzed by TLC on Silica Gel 60 (Macherey-Nagel) run in dichloromethane (4) followed by phosphorimaging (Variable Mode Imager Typhoon TRIO, Amersham Biosciences). The relative percentage of radioactivity incorporated in fatty acids (FA), in alpha-mycolic acids (α-MA) and in methoxy- and keto-mycolic acids (M+K MA, not separated during TLC) was determined for each condition using Image Quant 5.1 software.

Docking

Molecular graphics were performed with Accelrys Discovery Studio Visualizer (Accelrys Software Inc., Discovery Studio Modeling Environment, Release 4.0, San Diego: Accelrys Software Inc., 2013).

The compounds of this study were thoroughly built and fully optimized before the docking stage using the PM6 Hamiltonian (5) implemented in the MOPAC 2012 quantum chemistry package (6). In most cases a chiral center was present, both configurations *R* and *S* were taken into account.

The structure 2H7M from the Brookhaven Protein Data Bank was chosen for molecular docking. The NADH cofactor was kept into the InhA structure although 2H7M ligand and water molecules were removed. The MolProbity software (7) was used to assign the position of hydrogen atoms and the protonation state of histidines in the InhA protein.

The docking calculations were performed with the docking program Autodock Vina v1.1.2 (8). The Autodock graphical interface AutoDockTools (9) was used to keep polar hydrogens and add partial charges to the proteins using the Kollman United charges. The search space was included in a box of 24x24x24 Å, centred on the binding site of the ligands and nicotinamide cofactor. The side chains of the six residues, Met103, Phe149, Tyr158, Met161, Met199 and Leu218, which surround the catalytic cavity, were allowed to rotate during the docking. Flexible torsions of side chains and of ligands were assigned with Autotors, an auxiliary module of AutoDockTools. For each calculation, fifteen poses ranked according to the scoring-function of Autodock Vina were obtained (VINA score). The docking procedure was followed by a post-docking optimization with the PM6-DH2 (10) method implemented into the MOPAC 2012 quantum mechanical package (6). For that purpose, the docking poses were merged into the cavities of the corresponding InhA and the complexes were submitted to a minimization stage in which the ligand, a set of 12 residues (Met103, Phe149, Met155, Tyr158, Met161, Thr196, Met199, Ile202, Leu207, Ile215, Ley218 and Glu219) delimiting the binding pocket and the totality of hydrogen atoms were fully energy-minimized. The remaining residues were kept frozen. The

localized molecular orbital method (keyword MOZYME) which was developed to enable calculation on large systems such as enzymes was applied (11). The effects of the solvation interface were simulated with the continuum model COSMO (12) with a dielectric constant set to 78.4. The interaction energies (E_{opt}) were calculated with the equation: $\Delta E = \Delta_f H$ (ligand-receptor complex) - $\Delta_f H$ (ligand alone) - $\Delta_f H$ (receptor alone).

Results and discussion

Chemistry

Based on our previous results showing that the C7 hydroxyl group and the lipophilic thiododecyl chain bound to the ring C of the azaisoindolinone scaffold are essential elements for the InhA inhibitory activity, the first strategy adopted in this work was to maintain intact these two elements and to carry out modifications on the azaisoindolinone framework namely on the ring A and on the hemiamidal cycle B. For this purpose, the pyridine ring (ring A) of the azaisoindolinone scaffold was substituted by a phenyl, an aminophenyl and a *N*-oxide pyridyl cycles (the latter coupled with a sulfur oxidation of the chain giving the corresponding sulfone). The hemiamidal cycle B was also modified at the N8 position by subsequent introduction of a hydroxyl or a methoxy group. In a second stage, replacement of the dodecylthiophenyl motif (ring C) by an alkyl triazole ring was performed *via* Huisgen-type cycloaddition. Finally, a ring extension of the hemiamidal 5-membered ring to a 6-membered pyridazinone-type ring was also performed. These chemical modulations are summarized in Figure 2.

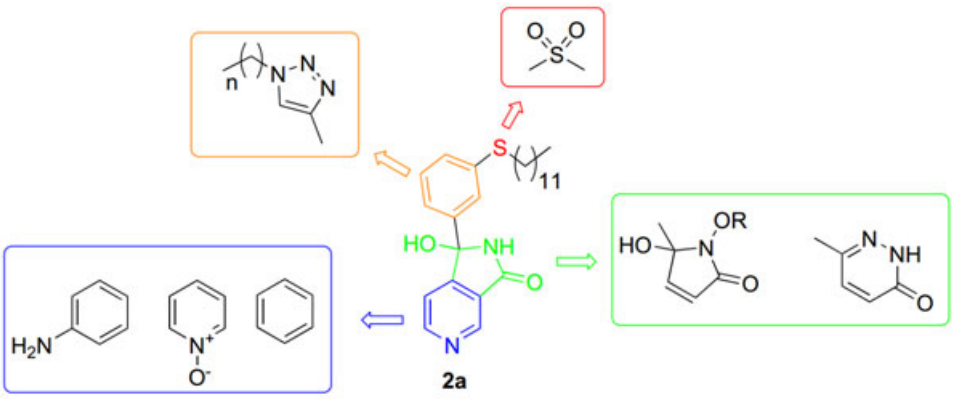

Figure 2. Structural evolution of azaisoindolinone scaffold **2a**.

The chemical synthetic routes of target compounds are presented in Scheme 1. The hit compound **2a** was synthesized according to our previously described procedure (2), which is

based on a nucleophilic addition of the dodecylthiophenyl lithium intermediate over the commercial 3,4-pyridine-dicarboximide reagent (**1a**). The introduction of the *N*-oxide motif into the hit molecule **2a** was carried out using *m*CPBA as oxidant (13). This reaction was accompanied by a subsequent oxidation of the sulfur atom leading to the sulfone **3**. The general synthetic strategy to prepare new compounds **2b**, **2c** and **4b** takes advantage of the addition of dodecylthiophenyl lithium intermediate upon dicarboximide starting materials embedding suitable functionalities (**1b**, **1c** and **1d** respectively). For the preparation of *N*-hydroxy or *N*-methoxy-(aza)isoindolinone derivatives **4a**, **5a** and **5b**, the synthesis initially consisted in the reaction of hydroxylamine or methoxylamine with (aza)phthalic anhydride **1e** or **1f** followed by addition of the aryllithium reagent (14). As previously observed for compound **1a** (15), the addition of the alkylthiophenyl group occurs preferentially on the *para* [a] carbonyl group and the regioisomers formed are readily separated by flash chromatography. Except for **4a**, whose the separation of isomers (ratio 70:30 *para*:*meta*) was not successful in these conditions and a HPLC preparative chromatography with a 2-ethyl-pyridine column was necessary. For **1c**, the exocyclic amine nitrogen atom oriented the reaction in a different way and promoted the addition on the *meta* carbonyl group with respect to the amino group. On the other hand, the replacement of the pyridine moiety by a phenyl ring suppresses the dissymmetry of the molecule discarding the formation of regioisomers during functionalization of the carbonyl group.

For the preparation of triazole compounds, addition of the lithium (trimethylsilyl)acetylide over the starting material **1a** and **1b** was carried out. After unsuccessful attempts on deprotection of the ethynyl group (due to the instability of the products), the intermediates **7a** and **7b** were directly submitted to a 1,3-cycloaddition reaction with the corresponding azides, which were prepared, in their tour, by reaction of NaN_3 with the corresponding halogen alkanes (16). The trimethylsilyl cleavage step was carried out by *in situ* addition of *tetra*butylammonium fluoride (TBAF) into the reaction mixture (17). This series of click-chemistry reactions led to a family of six compounds (**8a**, **8b**, **9a**, **9b**, **10a** and **10b**) by varying both aromatic ring A (phenyl /pyridyl) and the length of the alkyl chain (C_8, C_{10} and C_{12}).

Taking into account that pyridazinone compounds have potential antibacterial activities (18-21), the ring extension of the hemiamidal core of compounds **5a** and **5b** into pyridazinone **6a** and **6b**, respectively, was performed in good yield by using hydrazine under reflux (96% and 76% yield, respectively) (22, 23). Although this step is associated with the suppression of an

essential substituent (C7 hydroxyl group), this new scaffold has the advantage of deleting the asymmetric carbon.

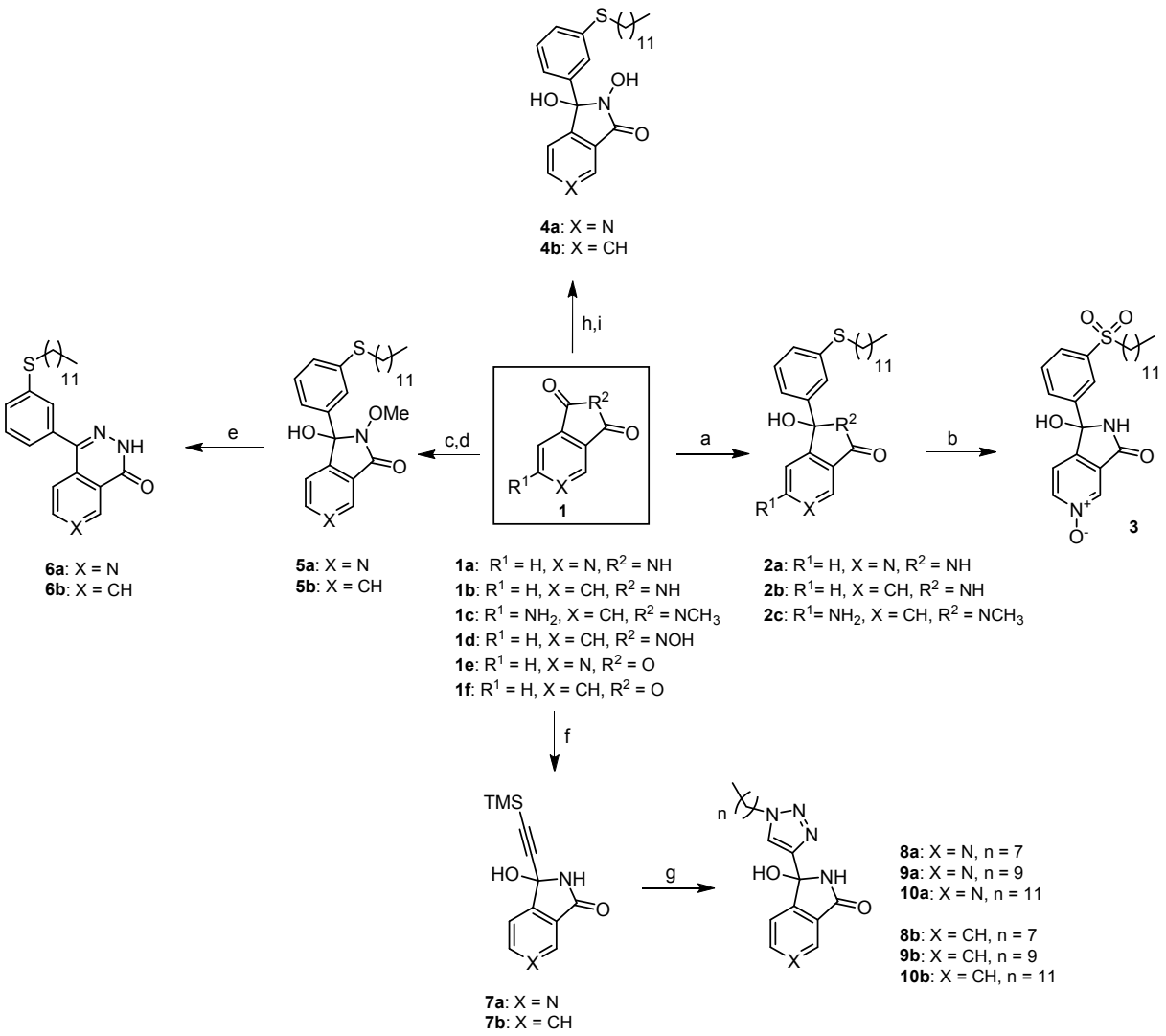

Scheme 1. Reagents and conditions: (a) $BrC_6H_4SC_{12}H_{25}$, *n*BuLi, THF, -78 °C, 37-58% (b) *m*CPBA, 72% (c) $H_2NOMe.HCl$, PTSA, toluene, reflux (d): $BrC_6H_4SC_{12}H_{25}$, *n*BuLi, THF, -78 °C, 26-36% (e) H_2NNH_2, EtOH, reflux, 76-99% (f): ethynyltrimethylsilane, *n*BuLi, -78 °C, 56-64% (g) $C_8H_{17}N_3$, $C_{10}H_{21}N_3$ or $C_{12}H_{25}N_3$, $CuSO_4.5H_2O$, NaAsc, EtOH, TBAF, 28-93% (h) for compound **4a**, $H_2NOH.HCl$, pyridine, reflux (i) $BrC_6H_4SC_{12}H_{25}$, *n*BuLi, THF, -78 °C, 30-44%

Enzymatic tests of InhA inhibition *in vitro*

The InhA protein was produced and purified according to a previous reported method (24). The compounds **2a**, **2b**, **2c**, **3**, ***p*-4a**, ***m*-4a**, **4b**, **5a**, **5b**, **6a**, **6b**, **8a**, **8b**, **9a**, **9b**, **10a** and **10b** (chiral molecules in racemic form) were evaluated for their InhA inhibitory activity by measuring the NADH consumption in the enzymatic reaction through the decrease of the absorbance at 340 nm. Target compounds were tested at 50 µM and for the more potent molecules also at 10 µM. The result is expressed as the percentage of inhibition of the InhA

activity for the indicated concentration. Triclosan was employed as a positive control and it induced a complete loss of InhA activity at 10 µM. The data are summarized in Table 1.

The hit compound **2a** was re-evaluated and it exhibited 28% inhibition at 50 µM confirming the magnitude of activity according to the previous reported results (2).

All new synthesized compounds were able to inhibit InhA activity *in vitro*. Compounds **3**, **5b**, **6b**, **8a**, **9b** and **10b** displayed InhA inhibitory potencies comparable to the hit molecule **2a**. Compounds **2b**, **5a**, **6a**, **9a** and **10a** were slightly more active than **2a**. The best inhibitors were compounds ***m*-4a** and **4b**, which displayed approximately the same percentage of InhA inhibition as **2a** for 5-fold lower concentration (entries 1, 7 and 8). In contrast, compounds **2c**, ***p*-4a** and **8b** showed poor InhA inhibition for this series.

Structure-InhA inhibition relationship

In vitro, the fully oxidized compound **3** bearing an *N*-oxide pyridine and a sulfone function displayed the same InhA inhibitory activity as the hit molecule **2a**. The presence of extra heteroatoms in the framework of the azaisoindolinone did not contribute to improve the interaction of compound **3** within the InhA active site.

The replacement of pyridine by a phenyl ring was well tolerated. In some cases, pyridine derivatives seem to be slightly better than phenyl derivatives (entries 9 and 10, 11 and 12, 13 and 14, 15 and 16, 17 and 18). This suggests that pyridine nitrogen atom may be engaged in key interactions within the binding pocket of the protein. Substitution of cycle A by the amino-phenyl ring led to a deep drop in activity (entry 3). However, no conclusions could be assessed on the influence of either the extra amino group or the N8-methyl bond. It is not clear whether this effect was due to the presence of the extra amino group or the presence of the methyl group (or even to both of them).

Modification of the hemiamidal core was also investigated. Insertion of a hydroxyl group at N8 revealed a significant enhancement of the inhibitory activity of the molecule toward InhA *in vitro*. Indeed, azaisoindolinone-based derivatives **4a** (*para* and *meta* 70/30 molar ratio) (entry 5) and **4b** (entry 8) exhibited about three times more inhibitory potency toward InhA than the lead molecule **2a** at 50 µM. This encouraging results observed with the mixture of two regioisomers (**4a**) led us to separate them by preparative HPLC to evaluate their activities separately. Surprisingly, the ***m*-4a** regioisomer was much more potent (entry 7) than the *para* isomer ***p*-4a** (entry 6). Both the hydroxylamino group and the position of the nitrogen atom on the pyridine ring were found to be critical for the activity of the molecule. In accordance with these observations, the replacement of the hydroxylamino group by methoxylamino group

significantly diminished the activity of **5a** and **5b** (entries 9 and 10 respectively). This result strongly supports the proposal that N8-OH may form hydrogen bond interaction into the active pocket of the InhA.

The replacement of the dodecylthiophenyl (ring C) by a dodecyltriazolyl moiety in the pyridine series led to a more active compound (**10a** entry 17) than the reference molecule **2a**. The positive effect exerted by the dodecyltriazolyl group in the place of the dodecylthiophenyl substituent on this scaffold may be explained by new hydrogen bonding possibilities afford by the heteroatoms of the aromatic cycle. Structure-InhA inhibitory activity exploration in the triazole series was also carried out by modifying the length of the aliphatic chain. As observed previously (2), it was shown that the length of the alkyl chain plays an important role to ensure efficient inhibitory activity toward the InhA protein (entries 13, 15 and 17).

The pyridazinone-type derivatives **6a** and **6b**, obtained from the ring expansion of the hemiamidal moiety, showed a significant improvement of the inhibitory InhA activity when compared to **2a**. In this example, it was also found that pyridine-based compound was more active than benzene-based compound (entries 11 and 12).

Molecular Docking

Molecular docking calculations were performed in order to simulate the possible binding modes of azaisoindolinone compounds in the active site of the InhA protein, to rationalize the structure-InhA inhibition relationship observed in this work, and to define essential structural features. Although several InhA crystal structures in complex with different inhibitors are available, we chose the crystal structure PDB ID 2H7M (25) as target for the docking study because, as previously reported by our group (26), this protein showed good ability to reproduce different modes of interaction of ligands with respect to the corresponding X-ray data. In addition, its crystal structure was solved in complex with the arylamide-type inhibitor **d11** with significant inhibitory activity (**d11**, IC_{50} InhA = 0.39 μM), and with a high-resolution 1.6 Å.

It is important to note that each compound with scaffold A, as defined in Table 1, is a chiral molecule (asymmetric carbon 7) and thus exists as a racemic mixture. Previous studies have shown that when R^2 = NH, a rapid racemization of C7 for both *R* and *S* enantiomers occurs in solution (2), probably through an open intermediate structure in equilibrium (27). Nevertheless, the cycle form (azaisoindolinone) is the unique form detected by NMR. Consequently, the enantiomers were not separated and the compounds were used as a

racemate in this work. However, the docking experiments were carried out for each individual enantiomer.

New compounds **2c(*R*)**, **2c(*S*)**, ***m*-4a(*R*)**, ***m*-4a(*S*)**, ***p*-4a(*R*)**, ***p*-4a(*S*)**, **5a(*R*)**, **5a(*S*)**, **10a(*R*)**, **10a(*S*)** were docked into the substrate binding site of the 2H7M protein in complex with NADH cofactor by using AutoDock Vina program. Due to their flexibility, these compounds show several combinations of conformation and orientation within the binding site. For each compound, the top-Vina score docking poses included into an interval of 2 kcal/mol energy were selected and were further subjected to an optimization step with the Hamiltonian method PM6-DH2 as previously described. Among the final possible conformations, we retained the ones that exhibited the lower optimized energy of interaction.

For comparison, we also show the orientation of the hit molecules **2a(*R*)** and **2a(*S*)**. The best binding mode predicted by docking calculations for different compounds is depicted in Figure 3.

The azaisoindolinone scaffold of **2a(*R*)** (Figure 3A) is located near the NADH cofactor and forms two hydrogen bonds between the carbonyl oxygen of the hemiamidal moiety and the C-2'-hydroxyl ribose of the nicotinamide nucleotide fragment and between the tertiary alcohol and one oxygen atom of the phosphate groups of the cofactor. This conformation shows the important role played by the tertiary alcohol in the binding of the active site and consequently, in the inhibitory activity of InhA which strengthens what has been previously revealed by the structure-activity relationship analysis (2). In the selected conformation of the **2a(*S*)** (Figure 3B), the azaisoindolinone scaffold is also located close of the NADH. However, the carbonyl group points to the opposite side of the cofactor and does not establish hydrogen bonds with it. In contrast, the pyridine ring is close to the Tyr158 and a hydrogen bond is observed between the hydrogen of the phenol function of the tyrosine and the pyridine nitrogen. In this conformation, the tertiary alcohol is also positioned in such a manner compatible with hydrogen bonding with one oxygen atom of a phosphate group. In both enantiomers of **2a**, the lipophilic chain occupies the top of the substrate-binding site.

The ***p*-4a(*R*)** and ***p*-4a(*S*)** (Figures 3C and 3D respectively) compounds are located globally in the same position as **2a(*R*)** and **2a(*S*)**, respectively and establish almost the same main interactions with the cofactor and the protein. It is interesting to note that, for regioisomers ***p*-4a(*R*)** and ***p*-4a(*S*)**, the *N*-hydroxylamine group was not responsible for additionnal interactions within the active site of the protein. In contrast, the *meta* regioisomer, compound ***m*-4a(*R*)** (Figure 3E), interacts with InhA by the two hydrogen bonds, which involve tertiary alcohol and carbonyl group, and a supplementary interaction between N8-OH and C2'-

hydroxyl ribose group. The other enantiomer ***m*-4a(*S*)** (Figure 3F) adopts in the active pocket of InhA an orientation allowing the establishment of four interaction points with the cofactor and the protein. These interactions take place between the tertiary alcohol at C7 and one of the phosphate oxygen, between the hydroxyl at N8 position and one of the saturated oxygen of the phosphate group, between the carbonyl group of the hemiamidal moiety and residue Thr196 and between the pyridine nitrogen atom and Tyr158 or C2'-hydroxyl ribose of the cofactor. All together, these interactions can account for a best activity observed for ***m*-4a** when compared to its regioisomer ***p*-4a** (entries 6 and 7).

Docking results revealed that compound **5a(*R*)** (Figure 3G) adopts a conformation in the InhA active site establishing two hydrogen bond type interactions as observed for ***m*-4a(*R*)**. However, different of ***m*-4a(*R*)** the N-OMe group is not able to interact with InhA nor NADH. On the other hand, the enantiomer **5a(*S*)** (Figure 3H) is positioned in a completely different manner. It is located far away from the NADH cofactor and hydrogen bonds with neither NADH nor Tyr 158 could be observed. We noted an unusual interaction between the tertiary alcohol at C7 and the Met 98. For compounds **10a(*R*)** and **10a(*S*)** (Figure 3I and 3J), the triazole ring is positioned near the Tyr158 and the ribose moiety. It is worth to note that, even in this case, the hydrogen bond between the tertiary alcohol at C7 and one of the oxygen atoms of the phosphate group is preserved. The location of the lipophilic chain is another difference between these compounds and **2a**. For compounds **10a(*R*)** and **10a(*S*)**, the chain is located in the bottom part of the cavity. Finally, the top Vina poses selected for **2c** (both *R* and *S* enantiomers), which is one of the less active compounds of the azaisoindolinone series, showed neither hydrogen bonding with NADH nor with Tyr158 (Figure 3K and 3L). Only the *S* enantiomer showed an uncommon interaction between the tertiary alcohol and the residue Met98. This lack of hydrogen bond interactions with the cofactor may explain the low inhibitory activity observed for this derivative.

In summary, binding modes allowing interactions with the nicotinamide nucleotide fragment (ribose and phosphate groups) of the cofactor NADH and with residue Tyr158 of InhA are always associated with inhibitory InhA activities *in vitro*.

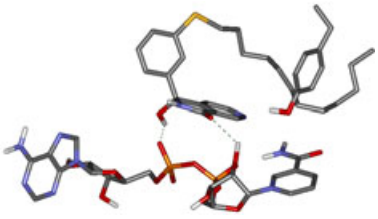

A. Vina = -9.5 kcal/mol

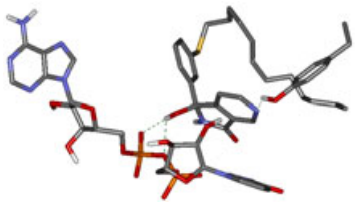

B. Vina = -9.6 kcal/mol

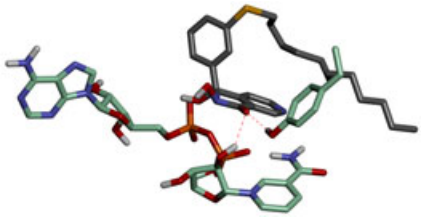

C. Vina = -9.6 kcal/mol

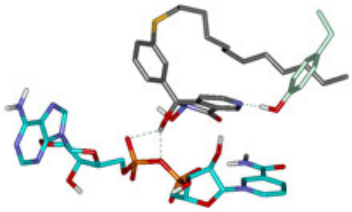

D. Vina = -8.8 kcal/mol

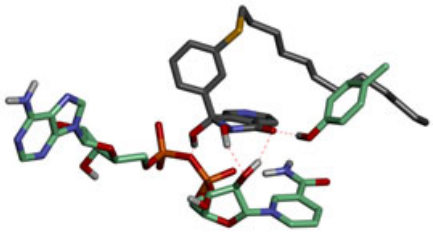

E. Vina = -9.5 kcal/mol

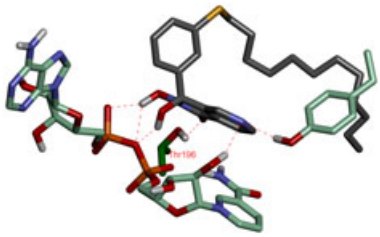

F. Vina = -9.3 kcal/mol

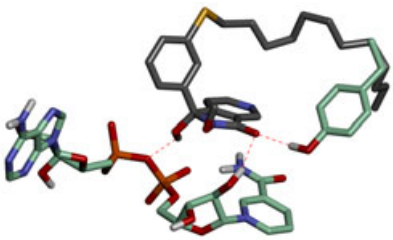

G. Vina = -9.3 kcal/mol

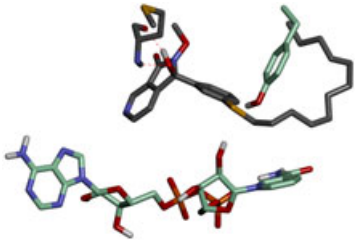

H. Vina = -8.6 kcal/mol

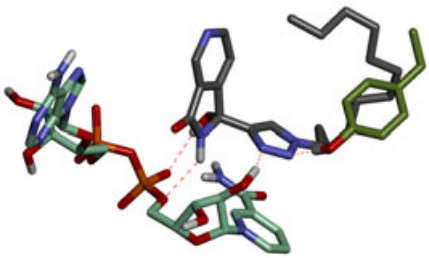

I. Vina = -9.6 kcal/mol

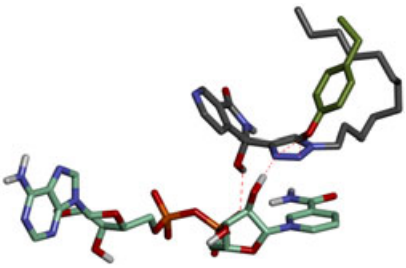

J. Vina = -9.5 kcal/mol

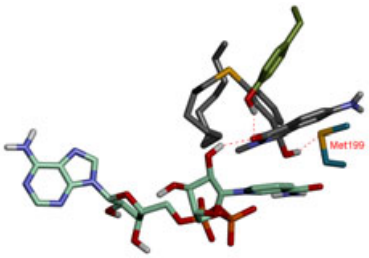

K. Vina = -8.8 kcal/mol

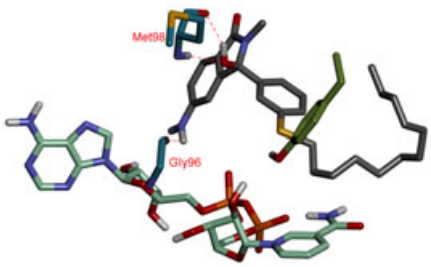

L. Vina = - 9.4 kcal/mol

Figure 3. The best binding modes of compounds **2a(*R*)** (**A.**), **2a(*S*)** (**B.**), **p-4a(*R*)** (**C.**), **p-4a(*S*)** (**D.**), **m-4a(*R*)**

(**E.**), **m-4a**(***S***) (**F.**), **5a**(***R***) (**G.**), **5a**(***S***) (**H.**), **10a**(***R***) (**I.**), **10a**(***S***) (**J.**), **2c**(***R***) (**K.**) and **2c**(***S***) (**L.**) predicted by docking calculations. Tyr158 residue and NADH cofactor molecule are respectively indicated as dark green and light green sticks.

Mycobacterium tuberculosis growth inhibition

In order to check whether the improved activity of InhA inhibiting of some compounds could be retrieved in the inhibition of Mtb growth, compounds **2a**, **3**, **4a**, **4b**, **5a**, **6a** and **10a** were evaluated toward inhibition of Mtb H37Rv growth using the same proceeding as reported in Menendez *et al* (28). The minimum inhibitory concentrations (MIC) were determined as the lowest drug concentration inhibiting bacterial growth. Triclosan was used as a positive control. The results are presented in Table 1. All tested compounds displayed an inhibitory activity toward *M. tuberculosis* growth globally equivalent to **2a**. Although compounds ***m*-4a** and **4b** were better InhA inhibitors *in vitro* than **2a**, they did not show however, higher inhibition potency toward Mtb growth.

Table 1. Effects of modifications upon the azaisoindolione framework on enzyme-inhibitory and antibacterial activities

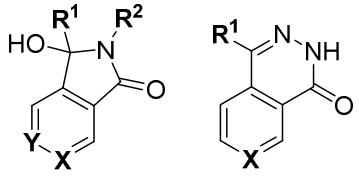

Scaffold A Scaffold B

Entry	Compound	Scaffold	R^1	R^2	X	Y	InhA inhibition (%)[a]		MIC (μM)[a] Mtb
							50 μM	10 μM	
1	**2a**	A	Ph-SC_{12}	H	N	CH	28.1 ± 1.1	-	23.4
2	**2b**	A	Ph-SC_{12}	H	CH	CH	42.4 ± 3.4	-	-
3	**2c**	A	Ph-SC_{12}	CH_3	CH	CNH_2	12.3 ± 4.6	-	-
4	**3**	A	Ph-$S(O_2)C_{12}$	H	NO	CH	34.6 ± 2.8	-	21.1
5	**4a**	A	Ph-SC_{12}	OH	N/CH	N/CH	76.1 ± 3.7	-	22.6
6	***p*-4a**	A	Ph-SC_{12}	OH	N	CH	11.4 ± 0.6	-	> 22.5
7	***m*-4a**	A	Ph-SC_{12}	OH	CH	N	80.1 ± 3.0	21	> 22.5
8	**4b**	A	Ph-SC_{12}	OH	CH	CH	81.6 ± 4.9	36	> 22.7
9	**5a**	A	Ph-SC_{12}	OMe	N	CH	42.8 ± 5.1	-	> 21.9
10	**5b**	A	Ph-SC_{12}	OMe	CH	CH	25.0 ± 5.2	-	-
11	**6a**	B	Ph-SC_{12}	-	N	-	57.8 ± 7.3	-	23.6
12	**6b**	B	Ph-SC_{12}	-	CH	-	30.7 ± 6.9	-	-
13	**8a**	A	Triaz-C8	H	N	CH	32.1 ± 0.8	-	-
14	**8b**	A	Triaz-C8	H	CH	CH	17.0 ± 1.7	-	-
15	**9a**	A	Triaz-C10	H	N	CH	45.4 ± 4.7	-	-
16	**9b**	A	Triaz-C10	H	CH	CH	31.3 ± 3.8	-	-
17	**10a**	A	Triaz-C12	H	N	CH	55.6 ± 4.4	-	26.9
18	**10b**	A	Triaz-C12	H	CH	CH	25.4 ± 1.2	-	-
19	**Triclosan**	-	-	-	-	-	-	97.5± 0.7	43

- not determined. a. All assays were repeated three times. b. All assays were repeated three times and standards deviations ± 0.025 mg/mL.

Inhibition of the mycolic acid biosynthesis

With these results in hands, it was the question whether the inhibition of Mtb growth by the synthesized compounds comes indeed from the inhibition of the InhA target. To answer to this question, we tested compounds ***m*-4a**, **2a** and INH, for comparison, toward the inhibition of mycolic acid biosynthesis in intact mycobacteria. Bacteria were treated at the MIC of each compound for 5 h and then incubated with [1-^{14}C]acetate for 18 h. After saponification, radiolabelled mycolic acids (MA) and fatty acids (FA) were analyzed as methyl esters by TLC and phosphorimaging. The results showed that, although these compounds inhibit InhA *in vitro*, they do not seem to target InhA inside *Mycobacterium tuberculosis* since they do not inhibit the mycolic acid biosynthesis in the used conditions. (Figure 4)

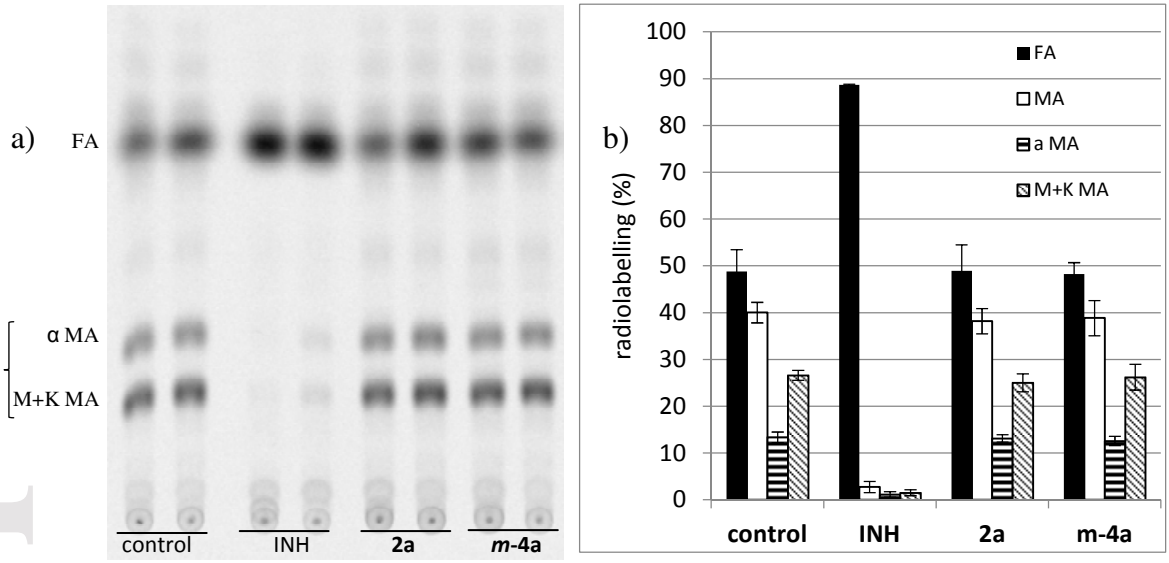

Figure 4. Effect of **2a** and ***m*-4b** on MA biosynthesis. Bacteria in culture were treated with either INH, **2a** or ***m*-4a** at their MIC and the neosynthesis of mycolic acids *in vivo* was followed by [1-^{14}C]acetate labelling (duplicates). a) TLC-phosphorimaging analysis of radiolabelled fatty acid and mycolic acid methyl esters. b) relative incorporation of radioactivity in various molecular species assessed on plate a). FA, fatty acid methyl esters; αMA, alpha-mycolic acid methyl esters; M+K MA, methoxy- and keto-mycolic acid methyl esters; INH, isoniazid.

Conclusion

A chemical modulation of the preceding azaisoindolinone-based compound **2a** was completed and 15 new analogues were synthesized and evaluated toward *in vitro* InhA inhibitory activity. Two of them, ***m*-4a** and **4b**, were more effective inhibitors than the hit molecule **2a** and inhibited about 80% of the InhA activity at 50 µM. Furthermore their mode of interaction with this enzyme *in vitro* was predicted based on molecular docking calculations and on the structure-inhibitory activity relationship analysis. This study aided us to define some critical interactions between possible inhibitors and the receptor. Indeed, the hydrogen bond interactions of inhibitors with the nicotinamide nucleotide fragment (ribose and phosphate groups) of the cofactor NADH and with residue Tyr158 of InhA are always associated with an inhibitory action. These compounds also exhibited an inhibitory activity upon *M. tuberculosis* H37Rv growth however, they were not able to inhibit the biosynthesis of mycolic acids in the studied conditions.

List of abbreviations

ACP = Acyl carrier protein
Asc = Ascorbate
DMSO = Dimethyl sulfoxide
HPLC = High-performance liquid chromatography
INH = Isoniazid
MA = Mycolic acid
m-CPBA = *meta*-Chloroperoxybenzoic acid
MDR = Multi-drug resistant strains
MIC = Minimum inhibitory concentration
Mtb = *Mycobacterium tuberculosis*
NADH = Chemical reduced form of nicotinamide adenine dinucletotide
PTSA = *para*-Toluenesulfonic acid
PIPES = Piperazine-*N*,*N*′-bis(2-ethanesulfonic acid)
TBAF = Tetra-*n*-butylammonium fluoride
TDR = Total drug resistant strains
TLC = Thin layer chromatography
TMS = Trimethylsilane

Acknowledgments

We thank the scientific council of the University Paul Sabatier by the doctoral fellowship of Aurélien Chollet.

Conflicts of interest

The authors declare no conflict of interests.

References

1. World Health Organization, Global Tuberculosis Report 2015 wwwwhoint/tb/publications/global_report/gtbr2015_executive_summarypdf?ua=1 (Accessed January 2016)

2. Deraeve, C., Dorobantu, I.M., Rebbah, F., Le Quéméner, F., Constant, P., Quémard, A., Bernardes-Génisson, V., Bernadou, J., Pratviel, G. (2011) Chemical Synthesis, Biological Evaluation and Structure-Activity Relationship Analysis of Azaisoindolinones, a Novel Class of Direct Enoyl-ACP Reductase Inhibitors as Potential Antimycobacterial Agents. Bioorg Med Chem;19: 6225–6232.

3. Delaine, T., Bernardes-Génisson, V., Quémard, A., Constant, P., Meunier, B., Bernadou, J. (2010) Development of isoniazid-NAD truncated adducts embedding a lipophilic fragment as potential bi-substrate InhA inhibitors and antimycobacterial agents. Eur J Med Chem;45: 4554-4561.

4. Daffé, M., Lanéelle, M.A., Asselineau, C., Lévy-Frébault, V., David, H. (1983) Intérêt taxonomique des acides gras des mycobactéries: proposition d'une méthode d'analyse. Ann Microbiol;134B: 241–256.

5. Rezac, J., Fanfrlik, J., Salahub, D., Hobza, P. (2009) Semiempirical quantum chemical PM6 method augmented by dispersion and H-bonding correction terms reliably describes various types of noncovalent complexes. J Chem Theory Comput;4: 1749-1760.

6. Stewart, J.J.P. Computational Chemistry, Colorado Springs, CO, USA, http://OpenMOPACnet

7. Chen, V.B., Arendall, W B I., Headd, J.J., Keedy, D A., Immormino, R M., Kapral, G.J., Murray, L.W., Richardson, J.S., Richardson, D.C. (2010) MolProbity: all-atom structure validation for macromolecular crystallography. Acta Crystallogr D. Biol Crystallogr;66: 12-21.

8. Trott, O., Olson, A.J. (2010) Autodock Vina: improving the speed and accuracy of docking with a new scoring function, efficient optimization, and multithreading. J Comput Chem;31: 455-461.

9. Morris, G.M., Huey, R., Lindstrom, W., Sanner, M.F., Belew, R.K., Goodsell, D.S., Olson, A.J. (2009) AutoDock4 and AutoDockTools4: automated docking with selective receptor flexibility. J Comput Chem;30: 2785-2791.

10. Korth, M., Pitonak, M., Rezac, J., Hobza, P.A. (2010) Transferable h-bonding correction for semiempirical quantum-chemical methods. J Chem Theory Comput;6: 344-352.

11. Stewart, J.J.P. (1996) Application of localized molecular orbitals to the solution of semiempirical self-consistent field equations. Inter J Quant Chem;58: 133-146.

12. Klamt, A., Schuurmann, G. (1993) Cosmo: a new approach to dielectric screening in solvents with explicit expressions for the screening energy and its gradient. J Chem Soc Perkin Trans II;799-805.

13. Jana, N.K., Verkade, J.G. (2003) Phase-vanishing methodology for efficient bromination, alkylation, epoxidation, and oxidation reactions of organic substrates. Org Lett;5: 3787–3790.

14. Nguyen, H.N., Cee, V.J., Deak, H.L., Du, B., Faber, K.P., Gunaydin, H., Hodous, B.L., Hollis, S.L., Krolikowski, P.H., Olivieri, P.R., Patel, V.F., Romero, K., Schenkel, L.B., Geuns-Meyer, S.D. (2012) Synthesis

of 4-Substituted chlorophtalazines, dihydrobenzoazepinediones, 2-pyrazolylbenzoic acid, and 2-pyrazolylbenzohydrazide via 3-substituted 3-hydroxyisoindolin-1-ones. J Org Chem;77: 3887–3906.

15. Broussy, S., Bernardes-Génisson, V., Quémard, A., Meunier, B., Bernadou, J. (2005) The first chemical synthesis of the core structure of the benzoylhydrazine-NAD adduct, a competitive inhibitor of the Mycobacterium tuberculosis enoyl reductase. J Org Chem;70: 10502–10510.

16. Pardin, C., Roy, I., William, D., Keillor, J.W. (2008) Reversible and competitive cinnamoyl triazole inhibitors of tissue transglutaminase. Chem Biol Drug Des;72: 189–196.

17. Boons, G., Friscourt, F. (2010) One-pot three-step synthesis of cycloaddition of azides with alkynes formed by a sonogashira cross-coupling and desilylation. Org Lett;12: 4936–49439.

18. Husain, A., Ahmad, A., Bhandari, A., Ram, V. (2011) Synthesis and antitubercular activity of pyridazinone derivatives. J Chil Chem Soc;56: 778–780.

19. Abubshait, S.A. (2007) An efficient synthesis and reactions of novel indolyl- pyridazinone derivatives with expected biological activity. Molecules;12: 25–42.

20. Sönmez, M., Berber, I., Akbaş, E. (2006) Synthesis, antibacterial and antifungal activity of some new pyridazinone metal complexes. Eur J Med Chem;41: 101–105.

21. Akbas, E., Berber, I. (2005) Antibacterial and antifungal activities of new pyrazolo[3,4-D]pyridazin derivatives. Eur J Med Chem;40: 401–405.

22. Wang, X., Salaski, E.J., Berger, D.M., Powell, D., Hu, Y., Wojciechowicz, D., Collins, K., Frommer, E. (2011) Structure-based design of isoindoline-1,3-diones and 2,3-dihydrophthalazine-1,4-diones as novel β-Raf inhibitors. Bioorg Med Chem Lett;21: 6941–6944.

23. Brzezinski, J.Z., Bzowski, H.B., Epsztajn, J.A. (1996) Concise regioselective synthesis of hydroxyazaisoindolinones and their conversion into pyridopyridazinones. Tetrahedron;52: 3261–3272.

24. Chollet, A., Mourey, L., Lherbet, C., Delbot, A., Julien, S., Baltas, M., Bernadou, J., Pratviel, G., Maveyraud, L., Bernardes-Genisson, V. (2015) Crystal structure of the enoyl-acp reductase of mycobacterium tuberculosis (InhA) in the apo-form and in complex with the active metabolite of isoniazid pre-formed by a biomimetic approach. Journal of Structural Biology;190: 328-337.

25. He, X., Alian, A., Stroud, R., Ortiz de Montellano, P.R. (2006) Pyrrolidine carboxamides as a novel class of inhibitors of enoyl acyl carrier protein reductase from Mycobacterium tuberculosis. J Med Chem;49: 6308-6323.

26. Stigliani, J.L., Bernardes-Génisson, V., Bernadou, J., Pratviel, G. (2012) Cross-Docking Study on InhA Inhibitors: A Combination of Autodock Vina and PM6-DH2 Simulations to Retrieve Bio-Active Conformations. Org Biomol Chem;10: 6341–6349.

27. Stigliani, J.L., Arnaud, P., Delaine, T., Bernardes-Génisson, V., Meunier, B., Bernadou, J. (2008) Binding of the tautomeric forms of isoniazid-NAD adducts to the active site of the mycobacterium tuberculosis enoyl-ACP reductase (InhA): A theoretical approach. J Mol Graph Model;27: 536–545.

28. Menendez, C., Chollet, A., Rodriguez, F., Inard, C., Pasca, M R., Lherbet, C., Baltas, M. (2012) Chemical synthesis and biological evaluation of triazole derivatives as inhibitors of InhA and antituberculosis agents. Eur J Med Chem;52: 275–283.

[a] The *para* carbonyl group is defined with respect to the nitrogen of the pyridine ring. The other carbonyl group is subsequently defined as *meta*.

Supporting information

Additional Supporting Information may be found in the online version of this article:

Appendix S1: Table of docking and post-docking interaction energies for all compounds.